Psychophysical characterization of single neuron stimulation effects in rat barrel cortex

DISSERTATION

zur Erlangung des akademischen Grades

d o c t o r r e r u m n a t u r a l i u m

Dr. rer. nat.

im Fach Biologie

eingereicht an der

Mathematisch-Naturwissenschaftlichen Fakultät I

der Humboldt-Universität zu Berlin

von

Diplom-Psychologe

GUY DORON

Präsident der Humboldt-Universität zu Berlin

Prof. Dr. Jan-Hendrik Olbertz

Dekan der Mathematisch-Naturwissenschaftlichen Fakultät I

Prof. Stefan Hecht, PhD

Gutachter/innen:

1. Prof. Dr. Michael Brecht

2. Prof. Dr. Benjamin Lindner

3. Prof. Dr. Matthew Larkum

Tag der mündlichen Prüfung: 03.06.2013

Psychophysical characterization of single neuron stimulation effects in rat barrel cortex

PhD candidate:

Guy Doron

Supervisor:

Prof. Michael Brecht

November 2012

Bernstein Center for Computational Neuroscience
Animal Physiology / Systems Neurobiology and Neural Computation
Humboldt University Berlin, Berlin, Germany

Table of Contents

List of Figures

List of Tables

1. Abstract

The action potential (AP) activity of single cortical neurons can evoke measurable sensory effects, but it is not known how spiking parameters and specific neuronal subtypes affect the evoked sensations. Here we applied a reverse physiology approach to investigate the relationship between single neuron activity and sensation. First, we provide a detailed description of the procedures involved in nanostimulation, a single-cell stimulation method derived from the juxtacellular labeling technique. Nanostimulation is easy to apply and can be directed to a wide variety of identifiable neurons in anesthetized and awake animals. We describe the recording approach and the parameters of the electric configuration underlying nanostimulation. While exact AP timing has not been achieved, AP frequency and AP number can be parametrically controlled. We demonstrate that nanostimulation can also be used to selectively inhibit sensory responses in identifiable neurons. Next, we examined the effects of AP frequency, AP number and spike train regularity on the detectability of single-cell stimulation in rat somatosensory cortex. For putative excitatory, regular spiking neurons detectability increased with decreasing AP frequencies and decreasing AP numbers. Stimulation of single putative inhibitory, fast spiking neurons led to much larger sensory effects that were not dependent on AP frequency and AP number. In addition, we found that spike train irregularity greatly increased the sensory effects of putative excitatory neurons, with irregular spike trains being detected in on average 8% of trials. Our data suggest that the behaving animal is extremely sensitive to cortical APs and their temporal patterning.

2. Zusammenfassung

Die Aktionspotential (AP) -Aktivität einzelner kortikaler Neurone kann messbare sensorische Effekte hervorrufen. Es ist jedoch nicht bekannt, wie die Parameter der AP-Sequenzen und spezifische neuronale Subtypen die hervorgerufenen Sinnesempfindungen beeinflussen. Hier haben wir einen 'Reverse-Physiology' Ansatz angewendet, um die Beziehung zwischen der Aktivität einzelner Neuronen und der Empfindung zu untersuchen. Zunächst wird der Prozess der Nanostimulation, eine von der juxtazellulären Markierungstechnik abgeleitete Einzelzell-Stimulationsmethode, detailliert beschrieben. Nanostimulation ist einfach anzuwenden und kann auf eine Vielzahl von identifizierbaren Neuronen in narkotisierten und wachen Tieren angewandt werden. Wir beschreiben die Aufnahmetechnik und die elektrische Konfiguration für Nanostimulation. Während eine exakte zeitliche Bestimmung der AP nicht erreicht wurde, konnten Frequenz und Anzahl der AP parametrisch kontrolliert werden. Wir zeigen, dass Nanostimulation auch angewendet werden kann, um sensorische Reaktionen in identifizierbaren Neuronen selektiv zu inhibieren. Als nächstes haben wir untersucht wie sich die Frequenz und Anzahl der AP sowie die Regelmäßigkeit der Pulsfolge auf die Detektion von Einzelzell-Stimulationen im somatosensorischen Kortex von Ratten auswirken. Für erregende regular-spiking Neuronen erhöhte sich die Nachweisbarkeit mit abnehmender Frequenz und Anzahl der AP. Die Stimulation inhibitorischer und schnell feuernder Neuronen führte zu wesentlich stärkeren sensorischen Effekten, die unabhängig von Frequenz und Anzahl der AP waren. Außerdem fanden wir heraus, dass Unregelmäßigkeiten in der Pulsfolge die sensorischen Effekte von erregenden Neuronen stark erhöhten. Diese Unregelmäßigkeiten wurden in durchschnittlich 8% der Durchgänge festgestellt. Unsere Daten deuten darauf hin, dass es bezüglich des Verhaltens eine große Sensivität für kortikale AP und deren zeitlichen Abfolge gibt.

3. Introduction

A fundamental goal of neuroscience is to elucidate the link between neural activity and sensation. This problem can be approached by classical recording techniques which describe how neurons respond to sensory stimuli. Indeed, the first recordings of action potentials in nerve cells already suggested strong correlations between neural activity and sensations (Adrian, 1919). However, because extracellular recording of neuronal activity is a correlational technique, establishing causal links between neural activity and sensation proved to be difficult. In order to establish causal links between neuronal activity and perception a reverse physiology approach can be employed, in which behavioral responses are analyzed in response to induction of cellular activity. Intracortical microstimulation was until recently the only method that enabled activation of localized populations of neurons and directly influencing sensory perception (Salzman et al., 1990; Romo et al., 1998; Afraz et al., 2006). Based on microstimulation evidence it has been suggested that a spike count code ('rate coding') in quickly adapting neurons may account for perceptual discrimination in the primary somatosensory cortex of primates (Luna et al., 2005).

In recent years substantial advances have been made towards directly linking single-cell activity and sensation. The interest in the meaning of single-cell activity has been ignited by converging evidence from several experimental approaches which suggested that neural activity is more sparse than previously thought (Hahnloser et al., 2002; Olshausen and Field, 2004; Greenberg et al., 2008; Huber et al., 2008; Wolfe et al., 2010). Following the pioneering work of Vallbo and colleagues (1984), a number of studies have demonstrated effects of single-cell stimulation of excitatory neurons in the intact animal on movement (Brecht et al., 2004; Herfst and Brecht, 2008), sensation (Houweling and Brecht, 2008) and brain state (Li et al., 2009), as well as effects of single-cell stimulation of excitatory or inhibitory neurons on network dynamics (Bonifazi et al., 2009; Papadopoulou et al., 2011; Kwan and Dan, 2012).

It is still unclear, however, how specific cell types and their precise discharge patterns generate sensations. A previous study provided evidence that individual neurons in the rat barrel cortex can have an impact on behavioral responses in a detection task (Houweling and Brecht, 2008). Here we applied single-cell stimulation in putative excitatory and inhibitory neurons to investigate how the number, frequency and regularity of evoked APs affect this relationship. Specifically we asked the following questions: Does the behavioral report of single-cell stimulation vary with the (i) frequency, (ii) number, (iii) regularity of evoked spikes, and (iv) the type of stimulated neuron (excitatory vs. inhibitory)?

3.1 The somatosensory cortex of the rat as a model for sensory information processing

Rats are nocturnal mammals belonging to the rodents order living in burrows. Thus, they are mostly relying on their tactile senses, in the form of a whisker system, in order to explore their environment and retrieve essential information about the world around them. The tactile somatosensory pathway from whisker to cortex in rats (Figure 1) presents a distinct system for exploring the relation between neuronal activity and behavior (Brecht, 2007; Petersen, 2007). Importantly, the whisker (or vibrissa), the tactile organ in the form of a specialized hair, is found only three synapses away from the relevant sensory cortex. The sensory pathway to the primary somatosensory cortex (S1) is initiated by whisker deflection which causes a stretching of the membrane of the infraorbital branch of the trigeminal nerve (ION) of the trigeminal ganglion (Lichtenstein et al., 1990). The trigeminal ganglion projects the brain stem nuclei (including the principle trigeminal nucleus [Pr5] and all subdivisions of the spinal trigeminal complex [Sp5]: spinal trigeminal nuclei oralis [Sp5o], interpolaris [Sp5i] and caudalis [Sp5c]) (Veinante and Deschênes, 1999), forming the first synapse. It then reaches the thalamic somatosenory nuclei (2nd synapse), which include the ventral posterior medial nucleus (VPm), the medial part of the posterior nucleus (Pom) and the reticular nucleus (Erzurumlu et al., 1980). The thalamic neurons project to S1. Interestingly, there are at least three parallel processing streams (Yu et al., 2006). These include the lemniscal pathway, from Pr5 brainstem nucleus to the VPm and from there massively to layer 4 of S1 (but also to layers 3, 5B and 6), which is involved in spatially encoded information processing (Armstrong-James and Fox, 1987), the paralemniscal pathway, from Sp5i through the Pom to S1, mainly to layer 1 and 5a (Ahissar et al., 2000), thought to transmit vibrissal information of frequency and velocity and the extralemensical pathway which emerges from the Sp5i to the VPm and ends in the septal regions of S1 (Pierret et al., 2000). The function of this parallel stream is uknown, but it is speculated it participates in gating sensory signals induced by self-initiated movements, for filtering redundant sensory information.

Another prominent feature of the somatosensory system is its unique anatomic and physiological organization of whisker representations along its stations. Namely, the mystacial pad on the rat snout shows highly organized pattern which is conserved along its relay stations on the opposite side of the snout throughout the afferent somatosensory pathway. These stereotypical cytoarchitectonic units are revealed using cytchorome oxidase stain and termed barrelettes in the trigeminal nuclei (Ma, 1991), barreloids in the VPm (Van Der Loos, 1976) and barrels in layer 4 of the primary somatosensory cortex (Woolsey and Van der Loos, 1970), therefore termed also the 'barrel cortex'. Remarkably, the barrel cortex contains representation of each vibrissa, where each stained spot or 'barrel' can be mapped according to a coordinate system consisting rows (depicted by letters from A to E from dorsal

to ventral) and columns or arcs (described by numbers from 1 to 7 from caudal to rostral) (Woolsey and Van der Loos, 1970; Welker, 1971, see also Figure 1). Furthermore, this somatotopic organization is also reflected by the physiological properties of the neurons within a specific barrel, which response most vigorously to stimulation of one single whisker and weaker responses to neighboring whiskers (Simons, 1978; Armstrong-James and Fox, 1987; Diamond et al., 1993). These remarkable anatomical and physiological features of the somatosensory system, in addition to the fact that whisking is a simple form of behavior easy to quantify, makes the somatosensory system an attractive model for quantification and analysis of neuronal mechanisms underlying sensory encoding and perception in the cortex.

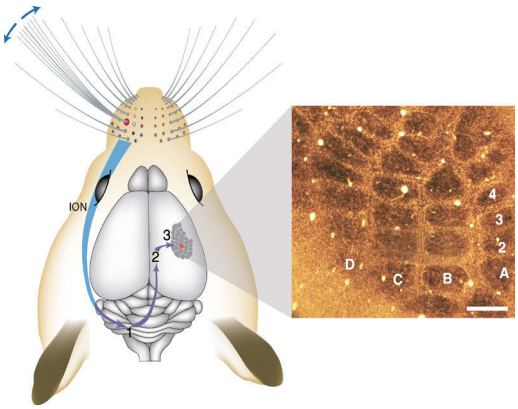

Figure 1: The leminscal pathway to somatosensory cortex. The whiskers on the snout are innervated by the infraorbital branch of the trigeminal nerve (ION), which transmits sensory information to the rostral principal nucleus (Pr5 [1]) in the brainstem. Trigeminothalamic axons from the Pr5 project to the ventral posteromedial nucleus (VPm [2]) in the thalamus in the contralateral hemisphere. Thalamocortical axons from the VPm project to the primary somatosensory cortex (S1 [3]). The arrangment of cortical barrels is shown on the right. Scale bar 200 µm. Modified from Knott et al., 2002.

3.2 Manipulating neural activity in cortices

Understanding the relationship between neural activity and percept is a fundamental goal of neuroscience. For decades, this issue was pursued by neural recordings in sensory cortices, which demonstrated that cortical activity signals abstract sensory features and is closely correlated to properties of sensory stimuli (Hubel and Wiesel, 1977). Subsequent works in behaving animals showed that such activity can even reflect the subjective judgments of an individual about stimuli (Britten et al., 1996). While recording studies established close correlations between neural activity and perception, the recording approach per se cannot tell us if a particular pattern of neural activity is sufficient for a certain percept. Thus, in order to establish causal relationships between neuronal activity and perception, it is essential to influence neuronal firing in the cortex, using an approach known as reverse physiology (Figure 2). The earliest neural stimulation technique used electrodes placed onto the surface of the brain. Hence, it was demonstrated for the first time that currents in the milliampere range can activate cortical tissue and thereby initiate movements (Fritsch and Hitzig, 1870) and later on even elicit sensory percepts in the brain (Penfield and Boldery, 1937), depending on the location of the electrode. The introduction of the microstimulation technique (Asanuma and Sakata, 1967) permitted

even a more precise spatial control of neural activation with currents in the microampere range. This technique proved successful in activation of local neuronal populations which led to movements (Asanuma, 1989) and artificial sensory percepts (Bartlett and Doty, 1980; Schmidt et al., 1996; Tehovnik et al., 2003; Butovas and Schwarz, 2007; Murphey and Maunsell, 2007). A breakthrough in the causal analysis of the neural underpinnings of perception came with the microstimulation studies of Newsome and colleagues (see Cohen and Newsome, 2004 for review). These microstimulation experiments in visual and somatosensory cortices established a direct link from sensory activity to behavior and suggested that small neuronal populations can influence sensory decisions (Salzman et al., 1990; Romo et al., 1998; de Lafuente and Romo, 2005; Afraz et al., 2006). In some of these studies behavioral responses produced by natural and artificial stimuli were indistinguishable (Romo et al., 1998). Microstimulation experiments, however, suffer from three major drawbacks: (i) the number of activated cells is unknown (Tehovnik 1995), (ii) the firing pattern of the activated cells is unknown, (iii) the identity of the stimulated cells is unknown. This lack of information calls for a development and implementation of novel methods which can provide data of single-neuron stimulation.

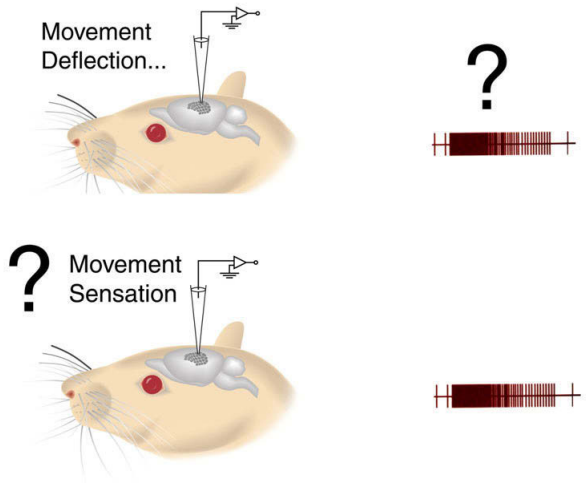

Figure 2: Classical versus reverse physiology approach.
The classical physiology approach (top) measures neuronal activity (e.g. spiking pattern) in response to external event (e.g., whisker deflection) and therefore reports correlations between these events and neuronal processing. In contrast, the reverse physiology approach (bottom) elicits neuronal activity (spiking pattern) and measures an overt behavior (movement, sensation) in response to such perturbations.

3.3 Sparse spiking in cortical neurons

The idea of sparse cortical neurons' discharge in higher brain areas was proposed four decades ago (Barlow, 1972). However, only in the last decade evidence started to accumulate regarding the

existence of possible sparse coding in the brain (Olshausen and Field, 2004; Brecht et al., 2005; Greenberg et al., 2008). The development of single-cell stimulation techniques provided evidence for the notion that the brain can compute using only a small but powerful sets of neurons (see Wolfe et al., 2010 for review). In-vivo studies in somatosenory and motor cortices, using patch-clamp recordings in anesthetized rats found that spiking activity is extremely low (Brecht and Sakmann, 2002; Margrie et al., 2002). Furthermore, evoking spikes in single motor cortex pyramidal neurons resulted in complex whisker movements (Brecht et al., 2004). The application of intracellular and whole cell recording techniques in anesthetized animals allowed also the identification of the stimulated neurons, however such recordings in the awake animals remained difficult to obtain (Steriade et al., 2001; Margrie et al., 2002; Crochet and Petersen, 2006; Lee et al., 2006). In order to deal with these complexities, juxtacellular stimulation has been used as an alternative in a variety of studies (Andrew and Fagan 1990; Brons et al. 1982; Cruikshank and Weinberger 1996; Fregnac et al. 1988, 1992; Lavallee and Deschenes 2004). Recently, a single-neuron stimulation study by Houweling and Brecht (2008) adopted this technique in order to examine the detectability of single neuron activity in the rat barrel cortex (Figure 3). In this study the authors trained rats to report cortical microstimulation. When they tested the animals by injecting minute currents using juxtacellular stimulation via a glass pipette, generating about 15 APs, they found that juxtacellular stimulation biased animals to report stimulation (through licking) more often than they did in catch trials lacking stimulation.

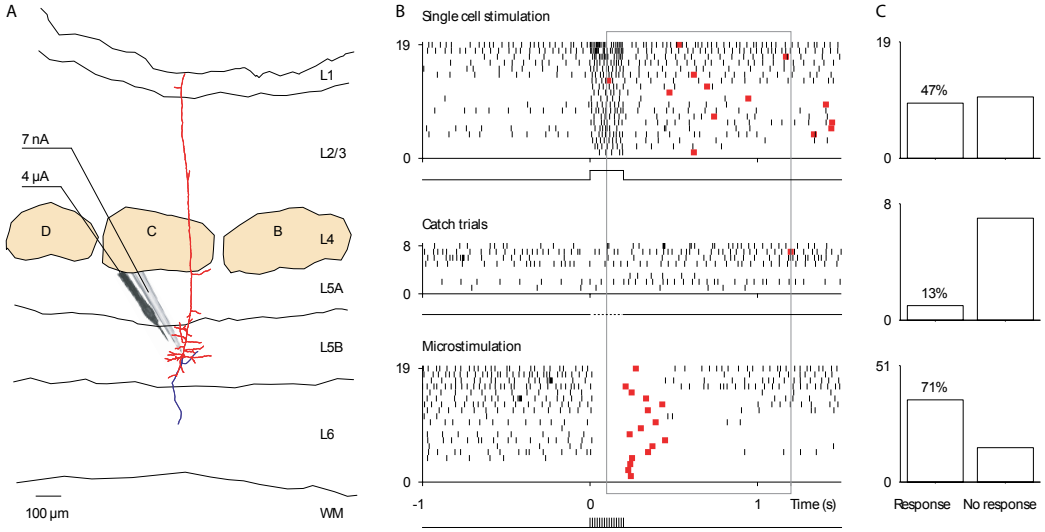

Figure 3: Behavioral report of single neuron stimulation in rat barrel cortex
(A) Reconstruction of the stimulated layer 5b pyramidal neuron with dendritic tree (red) and axon (blue, incompletely filled). Superimposed is a micrograph of a stimulation pipette and a tungsten microstimulation electrode aligned along the electrode track. Barrel rows (brown) are labelled with letters. L, layer; WM, white matter. **(B)** Action potential (ticks) raster plots and first lick responses (red squares) during juxtacellular single-cell stimulation trials (**top**), no-current-injection catch trials (**middle**) and 19 randomly selected microstimulation trials (**bottom**). The neuron was inhibited during and after microstimulation (stimulation current, 4 µA). **(C)** Quantification of responses to single-cell stimulation, catch trials and microstimulation. Adapted from Houweling and Brecht (2008).

Therefore they concluded that, at least under some circumstances, stimulation of just a single neuron in somatosensory barrel cortex can bias behavior. However, it is unknown how spike train parameters such as spike number, spike frequency or spike regularity affect detection behavior. In addition, it remains unclear whether specific cell types contribute differently to this phenomenon. In this work we extend this approach and also assess the effect of spike train parameters on single-neuron detectability. In addition we examine the role of specific cell types in this behavior.

4. Material and Methods

4.1 Animals

Male Wistar rats (n = 40, P33-P38 at the day of surgery) were obtained from Harlan (Horst, The Netherlands), housed with their siblings and maintained on a 12 hours light / 12 hours dark cycle with food and water ad libitum. Animals trained for the single-cell stimulation paradigm were housed in separate cages, handled and habituated to the experimental setup for 2-3 days before surgery. During the behavioral training and testing rats were kept under water control and had access to water during the experiment and one hour after the experiment. All experimental procedures were performed according to Dutch and German guidelines on animal welfare under the supervision of local ethics committees.

4.2 Surgical Procedures and Training

4.2.1 Acute experiments

For acute experiments, animals (n = 16) were anesthetized with urethane (1.5–2.0 g/kg ip). Glass pipettes for nanostimulation were filled either with intracellular solution containing (in mM) 135 K-gluconate, 10 HEPES, 10 Na_2-phosphocreatine, 4 KCl, 4 MgATP, and 0.3 Na_3GTP (pH 7.2). The juxtacellular signal was amplified and low-pass filtered at 3 kHz by a patch-clamp amplifier (Dagan, Minneapolis, MN) and sampled at 25 kHz by a Power1401 data-acquisition interface under the control of Spike2 software (CED, Cambridge, UK). Because nanostimulation elicits large DC shifts in the potential recorded during current injections, a digital DC remove filter was applied on-line (which subtracts at each point in time the average potential within $\Delta t = \pm 1$ ms) to allow monitoring of evoked APs. Series resistance and capacitance were not compensated.

4.2.2 Chronic experiments

All experimental procedures were performed as previously described (Houweling and Brecht, 2008; Voigt et al., 2008). Animals were implanted under ketamine/ xylazine anesthesia (100 mg/ kg, 5 mg/ kg, intraperitoneal, supplementary injections of ketamine or ketamine/ xylazine administered as needed) with a metal bolt for head-fixation and a recording chamber (P 2.5 mm, L 5.5 mm relative to bregma) for chronic access to barrel cortex. Over several days animals were habituated to head-fixation and a water restriction schedule with access to water ad libitum for one hour per day. Animals were then trained to respond with tongue lick to a 200 ms train of microstimulation pulses applied to barrel cortex (40 cathodal pulses at 200 Hz, 0.3 ms pulse duration) through a tungsten microelectrode and presented at random intervals. Tongue lick responses were detected with a beam breaker and rewarded during the task with a drop of saccharin water (0.1%), and counted as a hit if they occurred within 100

to 1200 ms after stimulus onset. The time of the first lick after stimulus onset was taken as the reaction time. To encourage animals to use a non-conservative response criterion, we only mildly punished licks in the interstimulus interval with an additional 1.5 s delay to the next stimulus presentation. The average interstimulus interval therefore depended on the frequency of interstimulus licks and measured 7.5 ± 2.4 s over all recording sessions.

4.3 Single-neuron stimulation detection task

Once animals performed at current intensities below 5 μA on two consecutive days we switched to single-cell stimulation experiments (Figure 4), as previously described (Houweling and Brecht, 2008; Voigt et al., 2008). Briefly, the animals were head-fixed during the task and waited for the microstimulation/ nanostimulation detection task to begin, when a neuron was found. During single-cell stimulation trials a 100, 200 or 400 ms square-wave current pulse was injected into a neuron through a glass pipette and current strength was adjusted (range 3-40 nA, median 12 nA) to elicit either a fixed number of APs at different duration for the AP frequency experiments or an increased number of APs using the same durations for the AP number experiments, without damaging the neuron. Single-cell stimulation trials, catch trials without current injection and microstimulation trials were pseudo randomly interleaved in series of 7 trials including 3 microstimulation trials, 3 single-cell stimulation trials (each of different duration) and 1 catch trial. All trials were presented at random intervals (Poisson process, mean 3 s). For the AP irregularity experiments, a 400 ms sequence was presented in order to induce an irregular spike pattern. It was comprised of 10, 20, 40, 80 and 160 ms step currents with intensities of 100%, 50%, 25%, 12.5% and 6.25%, respectively, that were randomly ordered along with a negative current pulse of 90 ms duration (at 50% of maximal current intensity), which served as inhibition pulse. In order to induce a regular spike pattern we used a single 400 ms current step. In another set of experiments determined to elicit burst like stimulation, brief stimulation duration of 25 ms was used, followed by 1175 ms inhibition at current intensities of 50% used in the nanostimulation, to prevent any further spikes during the stimulation trial. Microstimulation currents were adjusted (range 3-8 μA, mean 4.2 ± 1.1 μA (s.d.)) such that animals performed close to the detection threshold, resulting in an average microstimulation hit rate of 90%.

4.4 Electrophysiology

The glass pipette for juxtacellular single-cell stimulation and recording was glued to a tungsten microelectrode used for microstimulation at a distance of approximately 70 μm, as previously described (Houweling and Brecht, 2008; Voigt et al., 2008). The pipette was filled with intracellular solution

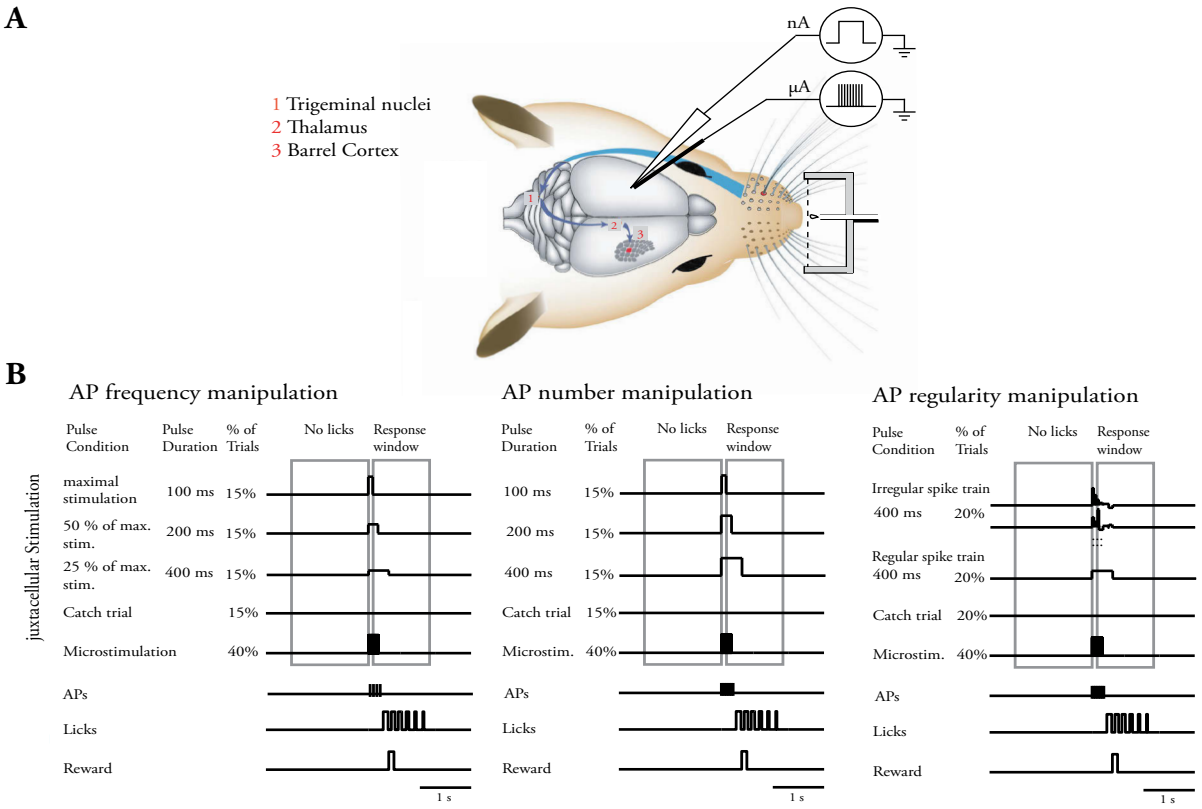

Figure 4: Stimulation protocols of parametric single-neuron stimulation
(A) Stimulation experiments were performed in the barrel cortex of awake rats. Animals responded to stimulation by interrupting a light beam (dashed line) with multiple tongue licks. The time of the first lick was taken as the reaction time and reward was delivered for correct responses (right). **(B) Left panel**, AP frequency manipulation: Five types of stimulus were presented at random intervals (Poisson process, mean 3 s): microstimulation (2–8 µA) (45% probability), 100 ms (max. current) juxtacellular single-cell stimulation (15%), 200 ms (50% of max. current) juxtacellular single-cell stimulation (15%), 400 ms (25% of max. current) juxtacellular single-cell stimulation (15%) and no current injection 'catch' trials (15%). Licks within the interstimulus interval led to an additional 1.5 s delay to presentation of the next stimulus (left box) and were rewarded after a stimulus (right box) for all trial types. **Middle panel**, AP number manipulation, same as Left panel, but juxtacellular single-cell stimulation condition consisted 100, 200 and 400 ms at constant frequency. **Right panel**, AP regularity manipulation. Four types of stimulus were presented: microstimulation (2 – 8 µA) (40% probability), 400 ms current step (regular stimulus, 20%), 400 ms stimulus comprised of 10, 20, 40, 80 and 160 ms step currents with intensities of 100%, 50%, 25%, 12.5% and 6.25%, respectively, that were randomly ordered along with a negative current pulse of 90 ms duration (irregular stimulus, 20%) and no current injection 'catch' trials (20%).

containing (in mM) K-gluconate 135, HEPES 10, Na2-phosphocreatine 10, KCl 4, MgATP 4, and Na3GTP 0.3 (pH 7.2). The juxtacellular signal was amplified and low-pass filtered at 3 kHz by a patch-clamp amplifier (Dagan, Minneapolis, MN) and sampled at 25 kHz by a Power1401 data acquisition interface under the control of Spike2 software (CED, Cambridge, UK).

Single-cell stimulation experiments were performed at a mean depth reading of 1554 ± 458 µm, which is likely an overestimate due to oblique penetrations and dimpling.

4.5 Histological analysis

Rats were sacrificed by an overdose of urethane or ketamine, and perfused transcardially with

0.9% phosphate buffer saline solution, followed by 4% paraformaldehyde in 0.1 m PB. Brains were removed from the skull and immersed in fixative for at least one day. To reveal the cell morphology of juxtacellularly-labeled cells, brains were sectioned in 150 μm thick coronal slices, which were then processed with the avidin-biotin-peroxidase method essentially as described previously (Brecht and Sakmann, 2002). Sections were then mounted with Moviol on glass coverslips. In most slices, additional cytochrome oxidase staining was performed to visualize the patchy organization of the barrel cortex. Neurons were reconstructed with Neurolucida software (MBF Bioscience, Williston VT, USA) and displayed as two-dimensional projections. In several cases, background from the biocytin stain made it difficult to recognize cytochrome oxidase patches directly adjacent to the neuron.

4.6 Data analysis

All reported values are expressed as mean ± standard deviation (s.d.) if not indicated otherwise. We restricted the analysis of behavioral responses to those single-cell stimulation and catch trials in which animals were considered attentive, as judged by their performance in microstimulation trials. Specifically, single-cell stimulation trials and catch trials were included if the animal responded in both the preceding and the succeeding microstimulation trial, or if the animal responded in a microstimulation trial that immediately preceded or succeeded the respective trial. A cell was included in the data set if at least five single-cell stimulation trials of each duration condition and five catch trials fulfilled this criterion. Reported single-cell stimulation and catch trial response rates therefore refer to these included trials. AP rates / numbers, however, were calculated over all trials. The average spontaneous firing rate was 5.1 ± 8.9 Hz (mean ± s.d.) for putative excitatory neurons and 10.8 ± 16.4 Hz for putative inhibitory neurons. This is a rather high spontaneous firing rate. We assume that two factors might contribute to high firing rates under our experimental conditions. First, we made no attempt to sample neurons in an unbiased way in our experiments and accordingly our audiomonitor was on during our search for cells; this may have resulted in sampling biases towards active units. Second, it seems likely that juxtacellular stimulation – which induces pores into the membrane of the cell under study and requires an extremely close approach – is stressful to cells and might possibly depolarize neurons and increase their spiking rate. In fact we observed slight increases in firing rates in several of our experiments (see our Figure 12, Figure 13 for examples). Since animals were awake and displayed movements during the task, single-cell stimulation experiments were typically of short duration (median 15, range 3.5-165 minutes). A median of 14 (range 5-197) single-cell stimulation trials conditions and 14 (range 5-196) catch trials were included per cell. For the burst-like experiment we counted only trials where at least one spike was evoked during the short stimulation step. A median

of 16 single-cell stimulation trials and 16 catch trials were included per cell. As we trained animals to report stimulation of the barrel cortex, we tested the prediction that single-cell stimulation led to responses (hits). Thus, differences between hit rates and false positive rates were evaluated using a one-sided, paired t-test as post-hoc test to evaluate the specific contribution of the nanostimulation condition, if necessary. The inclusion criteria for putative interneurons (fast-spiking [FS] neurons) were action potential width no greater than 0.4 ms and/or a response of at least 50 action potentials during at least one 200 ms current injection, as previously described (Houweling and Brecht, 2008). Spike width was defined as a spike's duration at spike amplitude, measured from threshold voltage (defined as the voltage at which the spike induced an inflection in the trace) to peak. The statistical difference between the putative excitatory and inhibitory groups we applied two-sided unpaired t-test. For the AP frequency, AP number and AP regularity experiment we used correlation measurements between the spiking parameter and behavioral effect size as well as t-test when needed. For the brief current experiments we applied two sided, paired t-test, as no prediction could be made on the directionally of the nanostimulation in these experiments. For the examination of single-neuron effects in individual cells of the irregular experiment we used the Freeman-Halton extension of the Fisher exact probability test for two-rows by three-column contingency table. For Local field potential (LFP) analysis juxtacellular signals were band-pass filtered at 4-30 Hz and a power spectrum histogram was calculated using Fast Fourier Transform (FFT) with Hanning window (of size of 0.65 s, 8192 bins of 1.5Hz, for frequencies between 0 and 12,500 Hz), for 2 s before stimulus start. The power spectrum was calculated separately for hits and misses for all single-cell stimulation trials and catch trials.

5. Results

5.1 Parametric control of spiking parameters using nanostimulation.

The purpose of this study was to examine the spiking patterns which underlie single-neuron detection in the rat barrel cortex. However, we first needed to examine whether juxtacellular stimulation can be used to parametrically control manipulation of single-neuron stimulation.

5.1.1 Recording approach

Nanostimulation is based on a commonly used procedure to stain individual neurons recorded extracellularly in vivo (Pinault, 1996). Using glass pipettes, Pinault showed that dyes such as biocytin enter a neuron if the pipette is close enough to fire the cell during alternating on/off 200 ms current injections of a few nA. To establish the juxtacellular configuration required for nanostimulation we use the following procedure. Neurons are searched for blindly using a glass whole-cell recording pipette (typical resistance 4-7 MΩ) while monitoring the pipette resistance using 1 nA current pulses (Figure 5A, 'Search'). Once the resistance reaches a certain level (typically 20 MΩ or above), the search pulse is switched off to check for the presence of APs indicating contact with a neuron. If APs remain smaller than 2 mV over a period of a few minutes, we move the pipette in small steps (2.5 μm) towards the neuron until the amplitude reaches 2 mV or larger (Figure 5A, 'Approach'). An attempt is then made to make the neuron fire short trains of APs by brief (200 ms) positive current injections of increasing strengths (Figure 5A, 'Entrainment'). Special care is taken to avoid signs of damage to the neuron (hyperpolarization shifts, AP broadening, strong reduction of AP amplitude during the current injection, or an increase in spontaneous activity), which may occur with current injections beyond those that elicit a maximum firing rate. Since nanostimulation elicits large DC shifts in the juxtacellular potential during current injections, a high-pass filter is applied to the recording to monitor the modulation of AP firing. If the neuron cannot be entrained, the pipette is advanced a few steps and the entrainment procedure is repeated. If entrainment fails or the neuron is lost the same pipette can be used to search for a new cell. Typical nanostimulation currents needed to modulate neuronal AP firing range between 3-30 nA. On average, 8.8 ± 5.6 (s.d.) nA is required to fire 8-12 APs in barrel cortical neurons (Figure 5B). The large DC potential shifts (and their equivalent transients in the high-pass filtered traces, indicated by triangles in Figure 5A) complicate the detection of spikes for a brief period of 1-2 ms at the onset and offset of current injections, and may result in a small underestimate of the total number of elicited APs (~1-2% for 200 ms current injections). There is an inverse relationship between the juxtacellular circuit resistance (total resistance measured by current

injections R_{total} – pipette resistance in the bath $R_{pipette}$) and the amount of current required to elicit a fixed number of APs (Figure 5B). This inverse relationship is predicted by the juxtacellular circuit diagram (Perkins 2006), from which it follows that the fraction of injected current that enters the cell equals $(R_{total}-R_{pipette})/(R_{patch}+R_{cell})$, where R_{cell} is the input resistance of the cell and R_{patch} the resistance of the small membrane patch directly underlying the tip of the pipette. There is also a negative correlation of spike height with the amount of current needed to elicit APs (Figure 5C). This latter dependence is surprising as there was no significant relationship between spike height and circuit resistance ($r = 0.26$, $p = 0.31$, t-test).

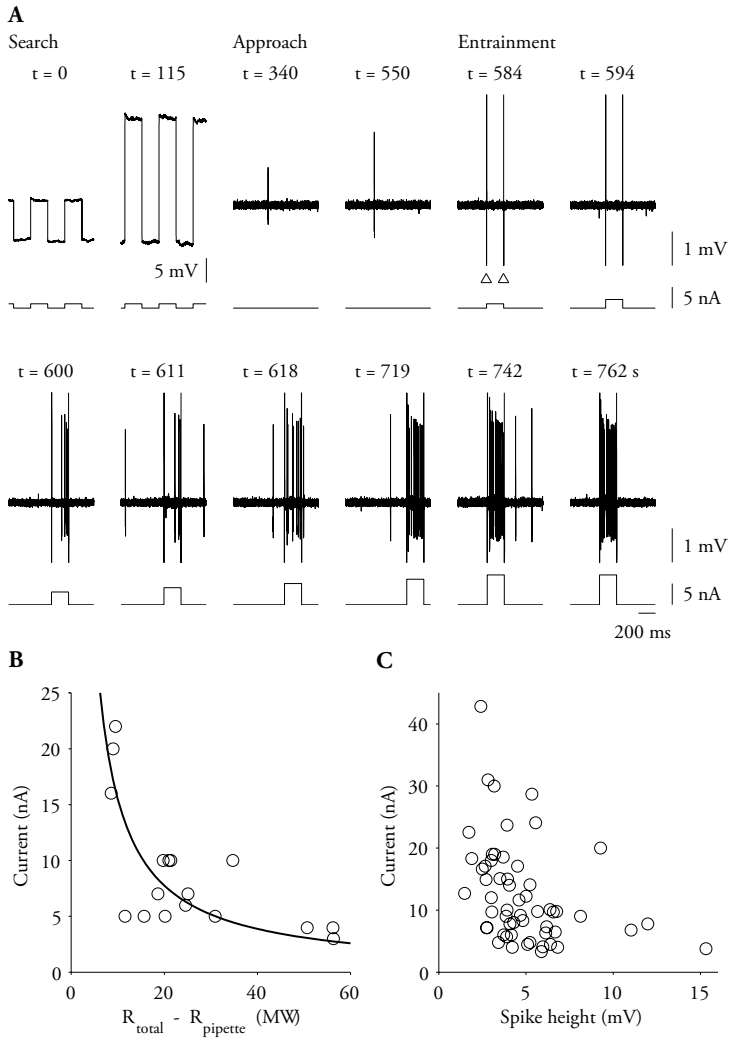

Figure 5: Nanostimulation procedure.
(A) Nanostimulation procedure illustrated in a barrel cortical neuron recorded in the awake headfixed animal. Upper traces display the juxtacellular potential ('search' phase) and which are high-pass filtered during 'approach' and 'entrainment' to monitor AP firing, while lower traces indicate current injection. During entrainment 200 ms current injections are repeated once every 5 s. Triangles indicate stimulation artifacts. **(B)** Relationship between total resistance of the juxtacellular circuit (Rtotal - Rpipette) and current intensity required to fire 8-12 APs in a series of experiments in the anesthetized animal (n = 17 cells). The black superimposed curve represents the theoretically expected relationship $y = c/x$, where c is a constant which was fitted to the data. **(C)** Relationship between AP height and average current intensity applied in barrel cortical neurons (n = 59) recorded in the awake behaving animal during a single-cell stimulation detection task (Houweling and Brecht, 2008).

In our view, perhaps the most important advantage of nanostimulation is that this technique is very easy to apply to a variety of preparations and neurons. Figure 6A illustrates our experimental setup for nanostimulation in the brain of chronically prepared animals. Much like tungsten microelectrodes, nanostimulation pipettes can be advanced through the intact dura (Figure 6B). The robustness of nanostimulation pipettes against minor mechanical obstacles like the dura and brain surface contaminations (as they typically occur in chronic preparations) is very different from in vivo whole-

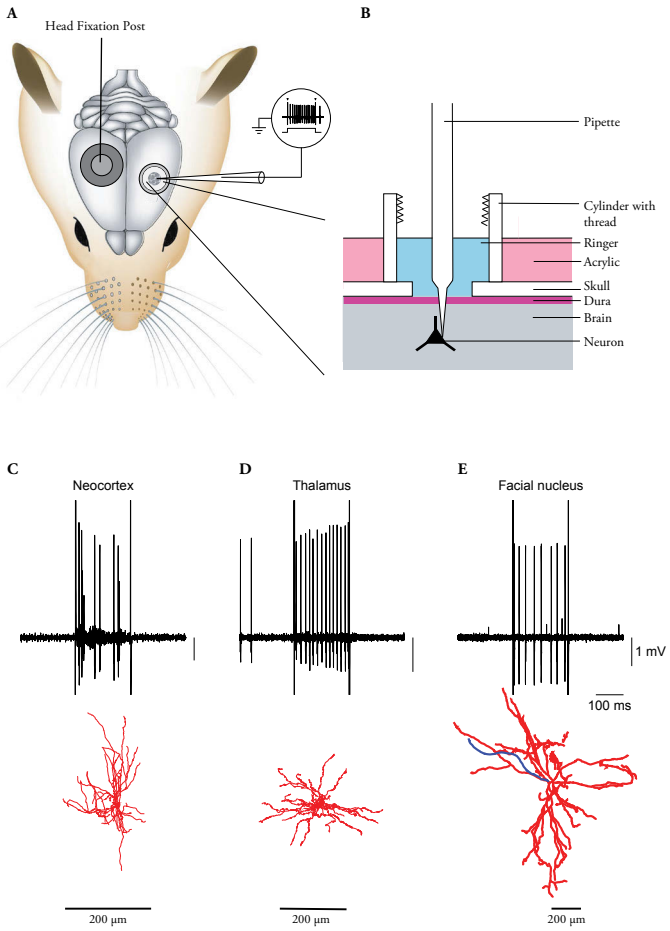

Figure 6: Nanostimulation setup and examples from different brain regions.
(A) Schematic (top view) of rat head with recording cylinder and head fixation post. **(B)** Schematic (side view) of the brain exposure and nanostimulation pipette in a chronically prepared animal. Nanostimulation examples from **(C)** barrel cortex, **(D)** thalamus and **(E)** facial nucleus. Reconstructed neurons are shown below the respective voltage traces.

cell recordings or sharp microelectrode recordings, which are greatly affected by such obstacles. As a consequence it is easy to target deep brain structures with nanostimulation pipettes – we never had a situation in which pipettes would break or irreversibly occlude in such experiments. Deep penetrations will result in damage to the overlying brain structures and for these applications it is useful to pull pipettes with long thin shanks. We have been able to apply nanostimulation to hundreds of neurons in widely different brain regions including the barrel cortex (Figure 6C, in this case a spiny stellate cell, one of the smallest cortical neurons), the thalamus (Figure 6D), and the facial nucleus (Figure 6E), which contains some of the largest neurons in the mammalian brain.

We assessed the stability of the nanostimulation configuration by quantifying the durations of nanostimulation sessions on 79 cells recorded in the barrel cortex of awake animals involved in a detection task (n = 8, unpublished data). For all these sessions a minimal number of each of several stimulation trial types had been presented satisfying an inclusion criterion for behavioral analysis (Houweling and Brecht, 2008). In this data set recording durations (i.e. elapsed time between first and last effective nanostimulation trial) ranged between 5-86 minutes, with an average duration of 22 ± 17 (s.d.) minutes and a median duration of 15 minutes. We did not collect detailed statistics on 'bad' recordings that did not satisfy our inclusion criterion. In these 8 animals, 79 successful recordings were obtained in 63 daily sessions (each lasting 2-3 hours), yielding an average success rate of 1.25 included cells per experiment.

To assess the health of neurons during the course of a nanostimulation experiment, we quantified spontaneous activity during experiments on neurons recorded in the barrel cortex (n = 70) and

visual cortex (n = 20) of awake animals involved in a detection task (Houweling and Brecht, 2008). Spontaneous firing rates were quantified in 1 s blocks preceding nanostimulation trials (see Figure 1d, Houweling and Brecht, 2008). In 13 out of 48 neurons (27%) for which recording durations exceeded 10 minutes, mean spontaneous activity during the 5-10 minute period following the first nanostimulation trial was significantly altered compared to the initial 0-5 minute period (shuffle test, $\alpha = 0.05$). In 2 out of 48 neurons (4%) spontaneous rates decreased (on average 1.3 spikes/s), and in 11 neurons (23%) spontaneous rates increased (on average 2.4 spikes/s). For the remaining cells that displayed stable spontaneous firing rates during the first 10 minutes and for which recording durations exceeded 20 minutes, mean spontaneous activity during the 15-20 minute period following the first nanostimulation trial was significantly altered in 5 out of 17 neurons (29%) compared to the initial 0-5 minute period. In 1 out of 17 neurons (6%) spontaneous rates decreased (2.5 spikes/s), and in 4 neurons (24%) spontaneous rates increased (on average 3.6 spikes/s). Thus, in a fraction of neurons small changes in spontaneous firing rate may accompany nanostimulation experiments. It must be noted however that many factors may have contributed to the observed changes in spontaneous firing rates over the course of these behavioral experiments, including changes in arousal state and possible long-lasting effects of nearby microstimulation on circuit organization.

In our experiments we used sustained DC current injections and consistently found that such prolonged current steps do not allow for a precise control of spike timing (Figure 7). Typically, AP firing is uniformly distributed over the nanostimulation interval (Figure 7A). Current injections that elicit an equal number of APs produce a large trial-by-trial variation in the timing of individual spikes (Figure 7B), even when the evoked spike trains are aligned on their first APs (data not shown). A variety of discharge patterns have been observed, including adapting spike trains reminiscent of regular spiking pyramid cells. Some control of spike timing may be obtained by restricting current injections to

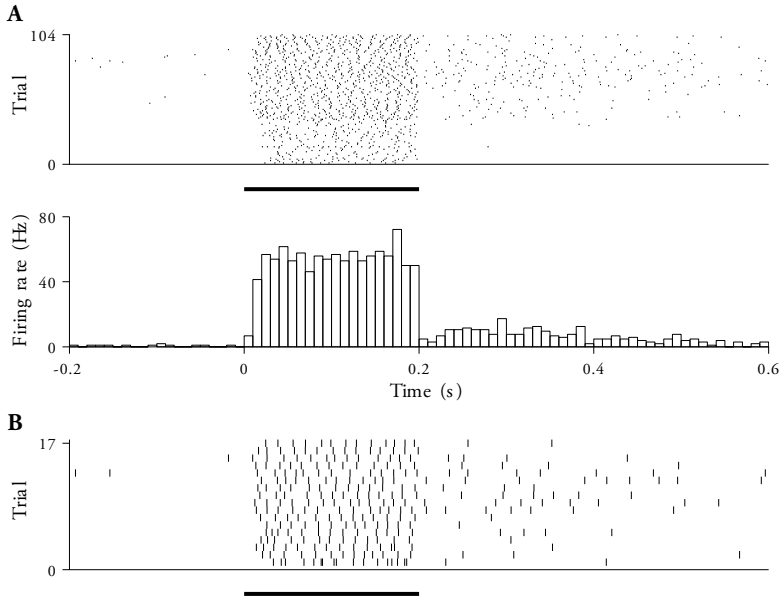

Figure 7: Spikes elicited by nanostimulation occur randomly during the injection interval.
(A) Spike raster plot (top) and post-stimulus time histogram (bottom) of a barrel cortex neuron recorded in the awake behaving animal. **(B)** Raster plot of the subset of trials in which exactly 13 APs were evoked during current pulses of 10 nA.

short pulses, although elicited APs are difficult to detect because of the large stimulation artifacts that last 1-2 ms (data not shown). In some cases AP firing is temporarily increased for a few hundred milliseconds following the end of the current injections (Figure 7A). These after-discharges can be prevented by a same size negative current injection directly following the positive current injection (data not shown).

5.1.2 Parametric control of AP frequency

To explore whether nanostimulation can be used to control AP frequency, we varied current intensity in barrel cortex neurons of anesthetized rats (n = 4). We first determined the maximal amount of current well tolerated by the cell by increasing the current to a point where further increases would jeopardize the viability of the recording. This current intensity (range 4-19 nA, mean 9.5 nA, n = 10 cells) elicited on average 13.3 ± 5.6 APs during 200 ms injections and we then applied 25, 50, 75 or 100 percent of this maximal current. In an experiment on a layer 6 inverted pyramidal neuron (Figure 8A), nanostimulation evoked on average 15 APs (i.e. 75 Hz) in response to the 100% current (8 nA) and proportionally fewer APs with 75%, 50% and 25% of the maximal current (Figure 8B, C). Average AP frequency varied linearly with nanostimulation current in the studied range for this cell (Figure 8C, $R^2 = 0.80$), as well as for our population of cells (Figure 8D). Although there was considerable variability in the evoked number of APs for a given current intensity, linear regression indicates that the control of AP frequency by varying nanostimulation intensity was good in all cells ($R^2 = 0.48$-0.97, median 0.73).

5.1.3 Parametric control of AP number

Next we determined whether nanostimulation can be used to control AP number. To this end we varied the duration of nanostimulation current applied to neurons in the barrel cortex of anesthetized rats (n = 6). Again, we determined a maximal stimulation current for each cell (range 3-30 nA, mean 9.7 nA, n = 12 cells). We then applied 50% of this current intensity for 100, 200, 400 and 800 ms durations. In a layer 4 pyramidal neuron (Figure 9A), 50% current intensity evoked on average 4 APs during a 100 ms current injection, and systematically more APs with longer stimulus durations (Figure 9B, C). The average AP number varied linearly with nanostimulation duration in the studied range for this cell (Figure 9C, $R^2 = 0.95$), as well as for our population of cells (Figure 9D). Although there was considerable variability in the evoked number of APs for a given current duration, linear regression indicates that the control of AP number by varying stimulus duration was good in all cells ($R^2 = 0.49$-0.98, median 0.90).

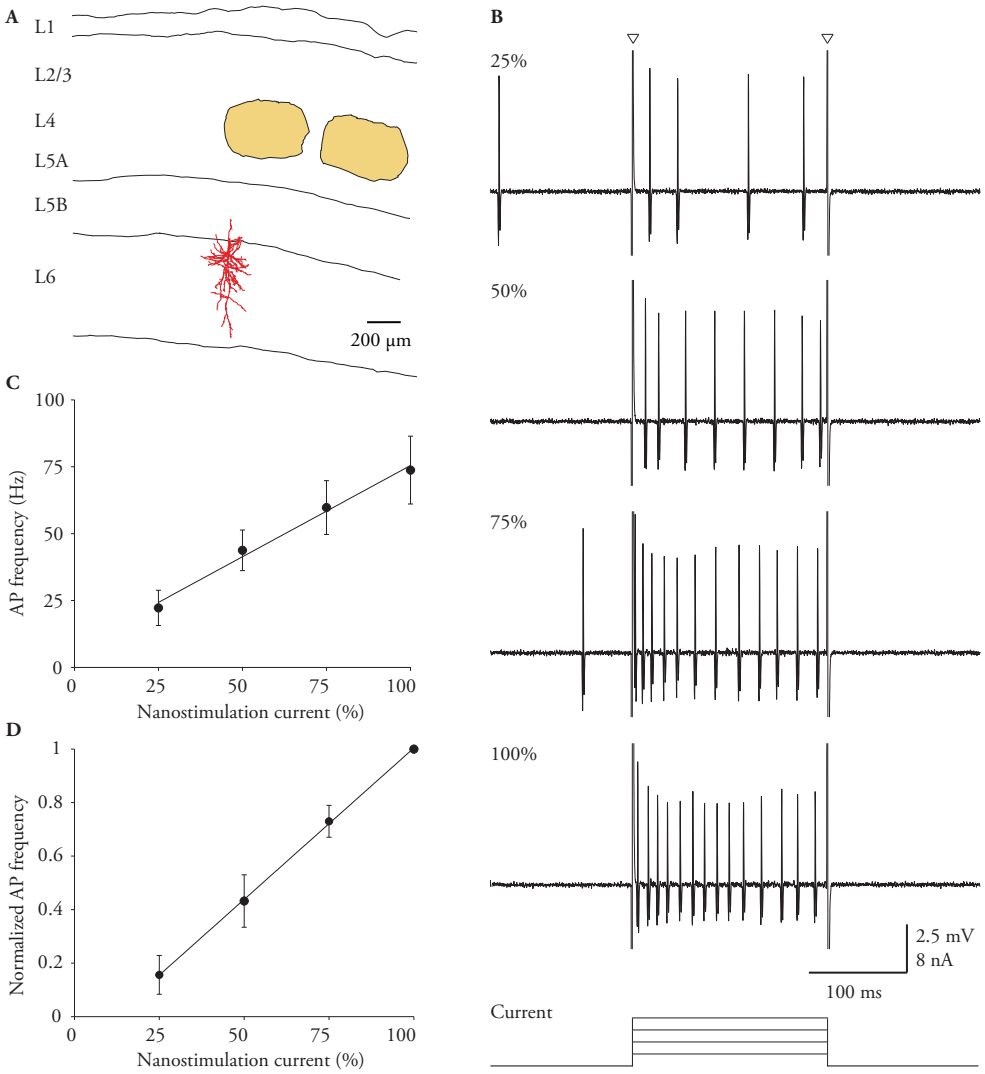

Figure 8: Effect of current intensity on spike frequency in barrel cortex neurons.
(A) Reconstruction of a stimulated layer 6 inverted pyramidal neuron with dendritic tree (black); axon was not filled and not reconstructed. Barrels are indicated in brown. L, layer. **(B)** Example AP discharges of the neuron for nanostimulation at different current intensities. Triangles indicate stimulation onset and offset artifacts. **(C)** Average AP frequency varied linearly with stimulus intensity in this neuron. **(D)** Population averages obtained by normalizing evoked AP numbers at 100% nanostimulation current. Error bars in **C** and **D** indicate standard deviations.

5.1.4 Inhibition of spiking activity

Finally we determined if nanostimulation could also be used for inhibiting AP activity. This feature is essential for eliciting irregular spiking patterns. We obtained sensory responses in 7 barrel cortex neurons of anesthetized rats (n = 6) by applying a 100 ms air puff to the whiskers. To inhibit AP firing we first determined a maximal stimulation current for each cell as before (range 5-16 nA, mean 9.1 nA) and applied the same intensity but as a negative current of 200 ms duration. We then presented air puff stimulation together with negative current injection and interleaved with air puff-only stimuli. As illustrated in Figure 10 for a layer 6 pyramidal neuron (Figure 10A), sensory AP

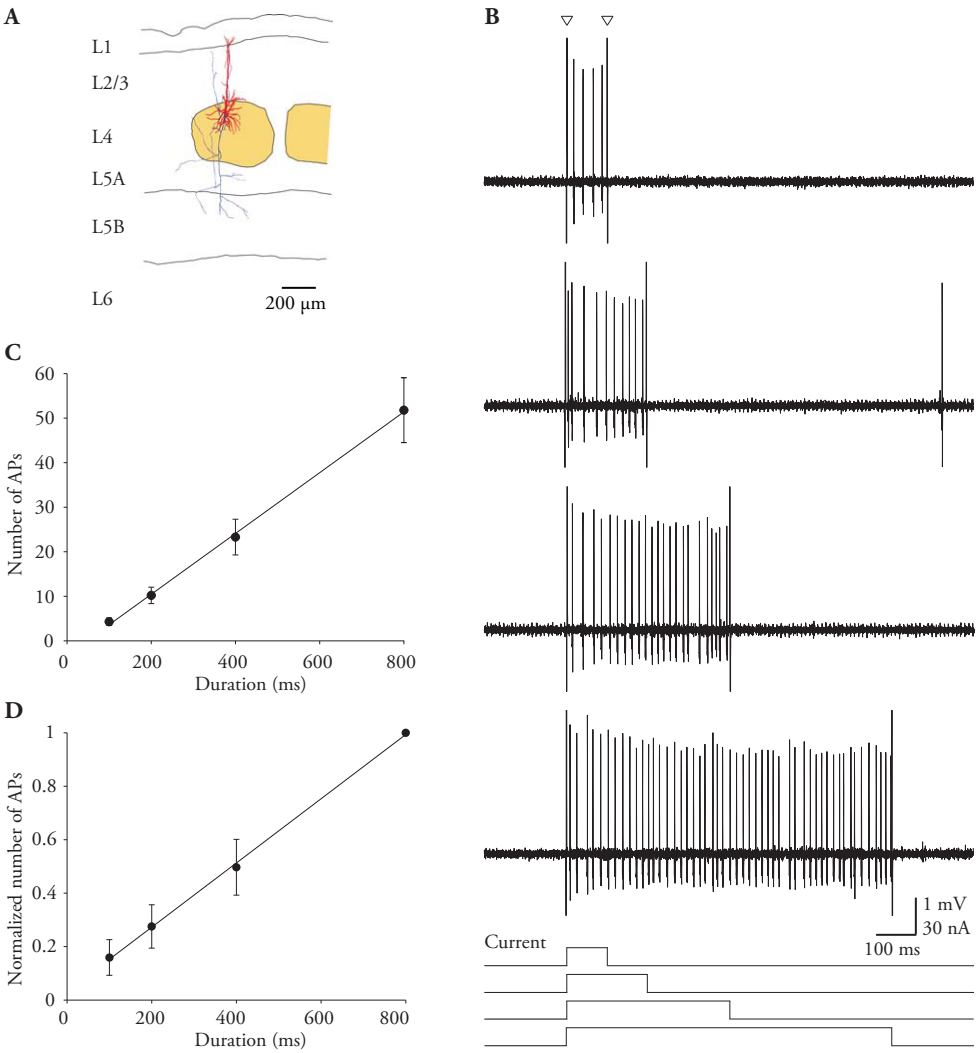

Figure 9: Effect of stimulus duration on spike number in barrel cortex neurons.
(A) Reconstruction of a stimulated layer 4 pyramidal neuron with dendritic tree (black) and axon (gray). Conventions as in Figure 8. **(B)** Example AP discharges of the neuron for nanostimulation at different durations. **(C)** Average AP number varied linearly with stimulus duration in this neuron. **(D)** Population averages obtained by normalizing evoked AP numbers at 800 ms stimulus duration. Error bars in **C** and **D** indicate standard deviations.

responses to the air puff (Figure 10B, top) were abolished when paired with a negative nanostimulation current (Figure 10B, bottom). Inhibition of sensory evoked activity was also clearly evident in the population averages (Figure 10C).

Because evoked AP frequency varies linearly with current intensity and AP number varies linearly with current duration, a stimulation protocol in which we vary current pulse intensity and duration together will result in stimulation trains of varying AP frequency and similar AP number. Similarly, a stimulation protocol in which we vary current pulse duration without changing current intensity will result in stimulation trains of varying AP number and similar AP frequency. Furthermore, adding negative current injection component to the current pulse pattern will result in more irregular stimulation trains. Hence, following the characterisation of this novel methodology we could now test it in the awake

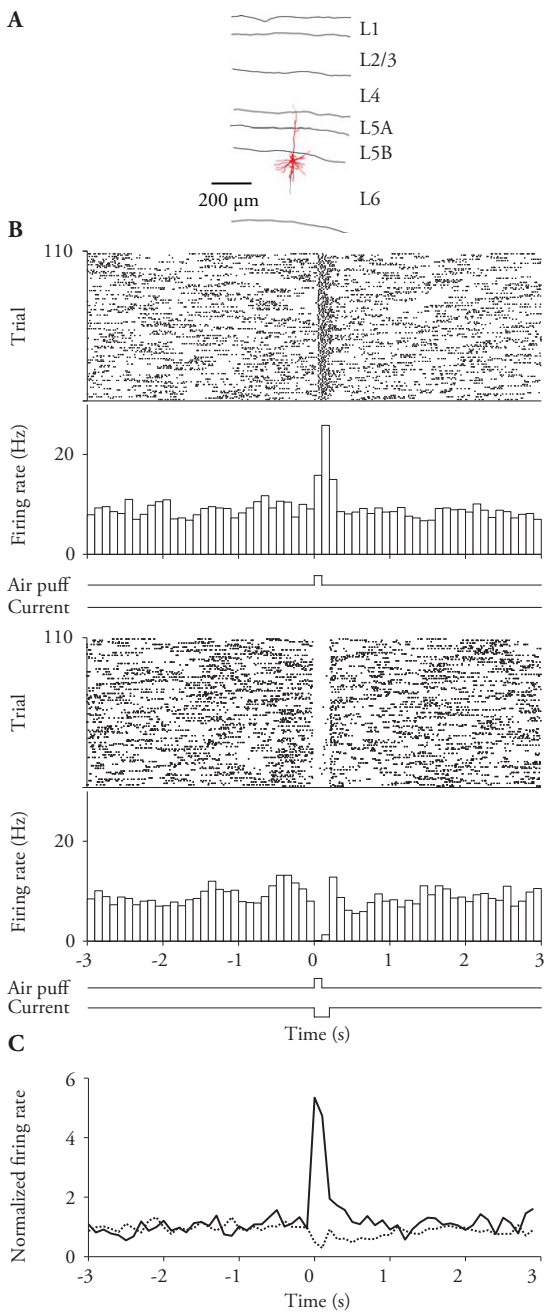

Figure 10: Negative current nanostimulation can prevent sensory responses in neurons of barrel cortex.
(A) Reconstruction of a stimulated layer 6 pyramidal neuron with dendritic tree (red) and axon (blue). Conventions as in Figure 8. **(B)** Spike raster plot and post-stimulus time histogram of the neuron while presenting air puff stimuli to the whiskers (top) and when paired with negative juxtacellular current injection (bottom). **(C)** Population averaged responses for air puff stimuli alone (solid line) and air puff stimuli paired with negative current injection (dotted line) (n = 7). Firing rates for each neuron were normalized using the baseline AP firing rate.

behaving rat during a detection task and examine whether different stimulation parameters result in a difference in the behavioural report of single neuron activity.

5.2 Effects of spike number, frequency and regularity on single neuron detectability

While it was shown that the activity of single cortical neurons can evoke measurable sensory effects, the relation between evoked sensations and AP frequency, number and spike train regularity, as well as the role of specific neuronal populations in this process remains unknown. Here we examined the effects of AP frequency, number and regularity on the detectability of single neuron stimulation in rat somatosensory cortex.

5.2.1 Putative inhibitory neurons are more detectable than putative excitatory neurons

Does the effect of single-cell stimulation depend on cell identity? We trained rats on a microstimulation detection task in which microstimulation (40 cathodal pulses at 200 Hz, 0.3 ms pulse duration) was applied to the barrel cortex. Tongue lick responses were rewarded with a drop of sweetened water and counted as a hit if a lick occurred within 100–1200 ms from stimulus onset. When the animals had reached their minimal detection thresholds (2-5 μA) after about one week of training, we then included additional trials in which we induced AP firing using nanostimulation, as described above, in order to manipulate of AP activity and identify individual neurons (Houweling et al., 2010), and applied to single cells recorded across all cortical layers.

To address if the sensory effects of single-cell stimulation were different for inhibitory and excitatory cells, we combined all data of our current experiments that contained 200 ms duration nanostimulation trials and those of a previously published study (Houweling and Brecht, 2008) (see Table 1).

Table 1: Experimental paradigms used in this study

Experiment	*Nanostim. duration (ms)*	*# Cells*	*# putative excitatory cells*	*# putative inhibitory cells*	*Figures*	*Included in meta-analyses*
Frequency	100/200/400	66	55	11	11-15	yes
Duration I	100/200/400	137	119	18	11,16-19	yes
Duration II	200/400/800	40	37	3	11, 18, 19	yes
Irregularity	400	74	62	12	20, 21	no
Brief 1-3 AP	25	41	30	11	22	no
Nature 2008	200	70	58	12	11, 14, 15, 18, 19	yes

We first classified our data set into fast-spiking (FS) interneurons, which we will refer to as putative inhibitory neurons, and non-FS neurons, which we will refer to as putative excitatory regular spiking (RS) neurons. The inclusion criteria were based on the evoked spiking pattern as illustrated in Figure 11A and B for traces from identified regular spiking and FS neurons. Cells were classified as FS if at least 50 APs were evoked during one or more 200 ms current injections and/ or if AP width was no greater than 0.4 ms (Houweling and Brecht, 2008). We verified some of the classifications by recovering and reconstructing excitatory (Figure 11C) and inhibitory (Figure 11D) cells. In 11 of 11 recovered cells the inclusion criteria correctly predicted excitatory (spiny / pyramidal, n= 9) and inhibitory (non-spiny, n= 2) neuron morphologies.

Comparing behavioral responses in single-cell stimulation trials (200 ms current steps) with no-

current-injection catch trials revealed a small but statistically significant difference in putative excitatory neurons (Figure 11E; average effect size 1.5%; P=0.04). In contrast, single-cell stimulation of putative

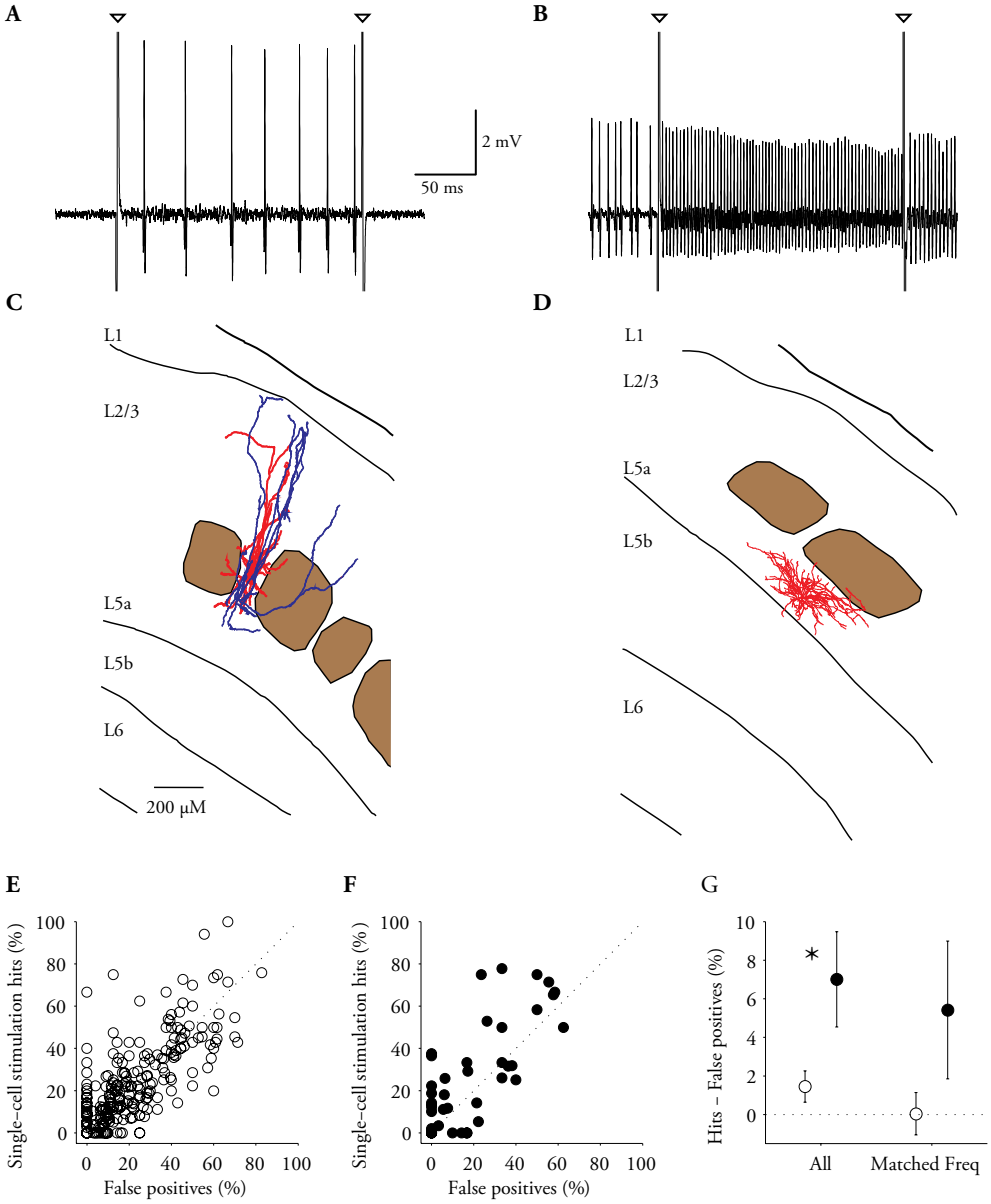

Figure 11: Stimulation of putative inhibitory neurons leads to stronger sensory effects
(A) Single-cell stimulation example trace of a regular-spiking, putative excitatory neuron. Triangles indicate stimulation onset and offset artifacts. **(B)** Single-cell stimulation example trace of a fast-spiking, putative interneuron. Conventions as in **A**. **(C)** Reconstruction of the dendritic (**red**) and axonal (**blue**) morphology of the putative excitatory cell from panel **A**, recorded from L4 during a single-cell stimulation experiment. **(D)** Reconstruction of the dendritic morphology of the putative inhibitory cell from panel B, recorded from L5 during a single-cell stimulation experiment. Conventions as in **A**. **(E)** Response rates for single-cell stimulation trials (hits) versus no-current-injection catch trials (false positives) of non-FS, putative excitatory neurons (**empty circles**; n=270 neurons; note several points coincide). one-sided paired t-test, P=0.04. **(F)** Response rates for single-cell stimulation trials (hits) versus no-current-injection catch trials (false positives) of FS, putative interneurons (**filled circles**; n=43 neurons; note several points coincide). one-sided paired t-test, P=0.004. **(G)** Comparison of sensory effects (single-cell stimulation hit rate - catch trial response rate) of non-FS and FS single-cell stimulation for all cells (left) and frequency matched cells (right). * two-sided unpaired t-test, P = 0.01.

inhibitory neurons led to much larger sensory effects (Figure 11F; effect size 7.0%; P=0.004) compared to putative excitatory neurons (Figure 11G; two-sided t-test, P=0.01). In addition, we compared behavioral responses in putative excitatory and inhibitory neurons at matched evoked AP frequencies. We selected all excitatory cells above their median evoked AP frequency (55 Hz) and all inhibitory cells below their median evoked AP frequency (111 Hz). Examining putative excitatory (n=135) and inhibitory neurons (n=21) at matched evoked AP frequencies (77 Hz and 79 Hz, respectively) revealed a similar difference in average effect size (0.04% vs. 5.4%, respectively) (Figure 11G). We conclude that the sensory difference between putative excitatory cells and inhibitory cells does not simply come about because we activated inhibitory cells more strongly, but that it results from a greater detectability of inhibitory cell spikes under our conditions.

5.2.2 Sensory effects vary with AP frequency in putative excitatory but not in inhibitory neurons

Does AP frequency influence behavioral performance in our single-cell stimulation detection task? To assess the sensory effects of spike frequency we performed experiments (n= 66 cells) in which we manipulated AP frequency in single-cell stimulation trials while keeping the number of APs fixed. Specifically, we selected a nanostimulation current intensity (11 - 17 nA, on average) that strongly discharged cells (13 ± 8 APs, mean ± s.d.) during 100 ms current injections (which we will refer to as the high frequency condition, 15% of all trials). In two other trial types we applied either 50% of this maximal nanostimulation current in a 200 ms step (the medium frequency condition, 15% of all trials) or 25% current intensity in a 400 ms step (the low frequency condition, 15% of all trials).

Because evoked AP frequency varies linearly with nanostimulation current intensity (Figure 8) this stimulation protocol resulted in stimulation trains of varying AP frequency and similar AP number. Note that although the evoked AP number was similar on average, it was susceptible to certain variability across trials. These nanostimulation trials were randomly interleaved with microstimulation trials (40% of all trials) and catch trials without current injection (15% of all trials), which were used to measure chance performance.

The result of such a single-cell stimulation experiment on a putative excitatory neuron is shown in Figure 12. Nanostimulation evoked on average about 13 APs in all three conditions (Figure 12A, B). Evoked AP frequency was 31 ± 23 Hz (mean ± s.d.) during the low frequency condition (Figure 12B top), 65 ± 30 Hz during medium frequency trials (Figure 12B 2nd from top) and 124 ± 50 Hz for the high frequency condition (Figure 12B middle). The animal in this experiment was highly conservative and reacted only once out of 11 catch trials without stimulation (Figure 12B 4th from

top; first lick responses are indicated by red squares). In comparison, the animal responded in a large fraction of microstimulation trials (Figure 12B, C bottom, 73%). For the nanostimulation trials lick responses occurred most often after low frequency stimulation (Figure 12B, C top), less often after medium frequency stimulation (Figure 12B, C 4th from top) and not at all following high frequency stimulation (Figure 12B, C middle).

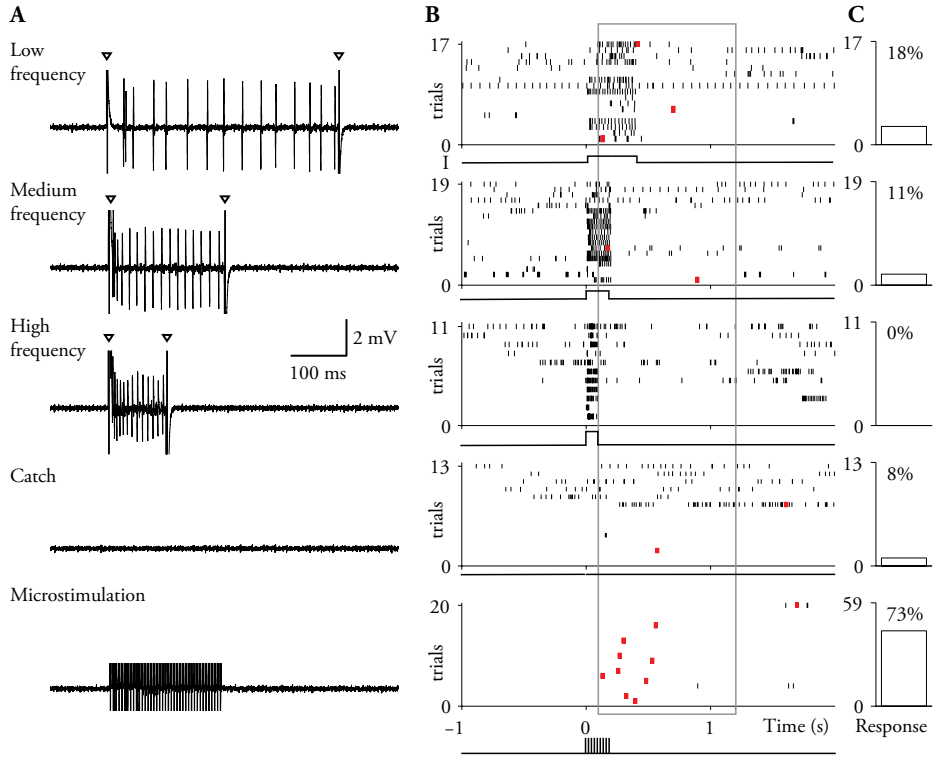

Figure 12: Behavioural responses to stimulation of a putatively excitatory neuron with different AP frequencies
(A) Recording of a putative excitatory neuron during low frequency (25% of maximal current), medium frequency (50% of maximal current), and high frequency (maximal current stimulation) nanostimulation, a no-current-injection catch trial and microstimulation. Triangles indicate stimulation onset and offset artifacts. In the microstimulation trace artifacts were partially clipped. **(B)** Action potential (ticks) raster plots and first lick responses (red squares) during the three different single-cell stimulation trials, no-current-injection catch trials and 20 randomly selected microstimulation trials (bottom). The neuron was inhibited during and after microstimulation (stimulation current, 4 µA). **(C)** Quantification of responses to single-cell stimulation, catch trials and microstimulation.

Figure 13 provides an example of a stimulation experiment with putative inhibitory neuron, in which we did not observe such an increase of sensory effect with decreasing AP frequency.

Because single-cell stimulation effects were relatively weak and trial numbers were typically low, the statistical significance of these effects was assessed at the population level (Figure 14). For putative excitatory cells there was a statistically significant negative correlation between AP frequency and the

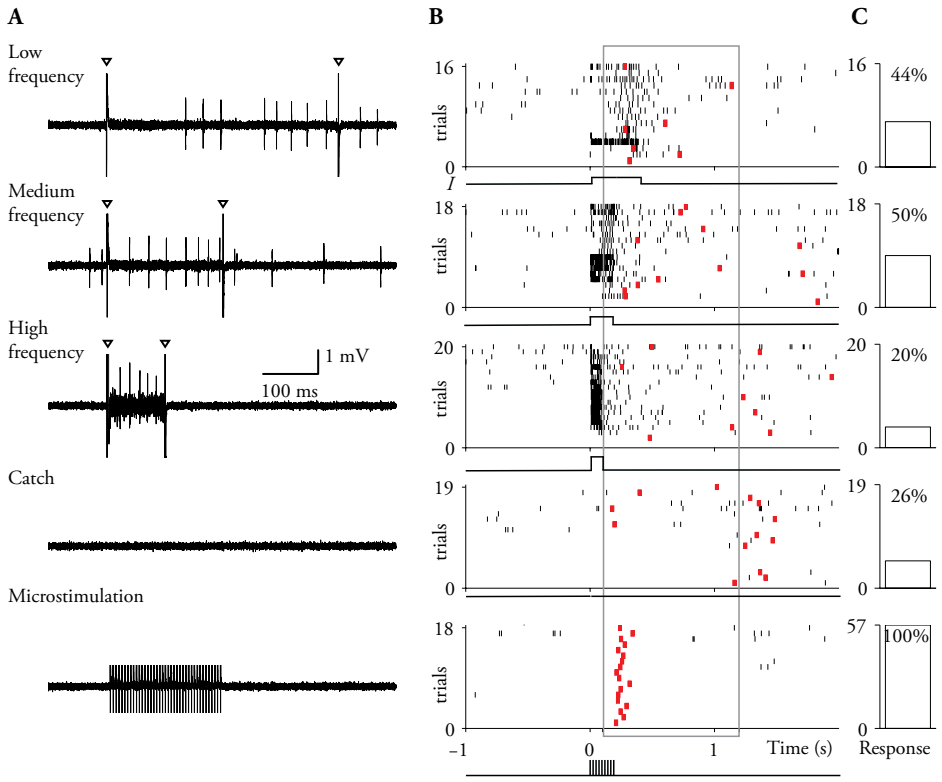

Figure 13: Behavioral responses to stimulation of a putative inhibitory neuron with different AP frequencies

(A) Single-cell stimulation example traces by juxtacellular current injection of low frequency (25% of maximal current, 48 ± 85 Hz), medium frequency (50% of maximal current, 94 ± 91 Hz), high frequency (maximal current stimulation, 191 ± 97 Hz), no-current-injection catch trial trace and microstimulation trial trace. Triangles indicate stimulation onset and offset artifacts. In the microstimulation trace artifacts were partially clipped. **(B)** Action potential (ticks) raster plots and first lick responses (red squares) during juxtacellular single-cell stimulation trials conditions, no-current-injection catch trials and 18 randomly selected microstimulation trials (bottom). The neuron was inhibited during and after microstimulation (stimulation current, 3 μA). **(C)** Quantification of responses to single-cell stimulation, catch trials and microstimulation.

detectability of single-cell stimulation (Figure 14A). We also examined the correlation between AP frequency and behavioral reaction times. Interestingly, our analysis revealed a statistically significant positive correlation between AP frequency and reaction times for putative excitatory neurons (Figure 14B). In addition, we examined the variance of the behavioral responses across stimulation conditions in the AP frequency experiment by binning all conditions into six equally sized groups according to frequencies. No significant relation between AP frequency and effect size variance was observed (Figure 14C). In contrast to putative excitatory neurons, no statistically significant correlation between AP frequency and sensory effect or reaction time was observed for putative inhibitory neurons (Figure 14D, E). In addition, no correlation between AP frequency and response consistency, as measured by the variance of the behavioral report across cells could be reported for these cells (Figure 14F).

In our experiments the absolute evoked AP frequency varied considerably from cell to cell.

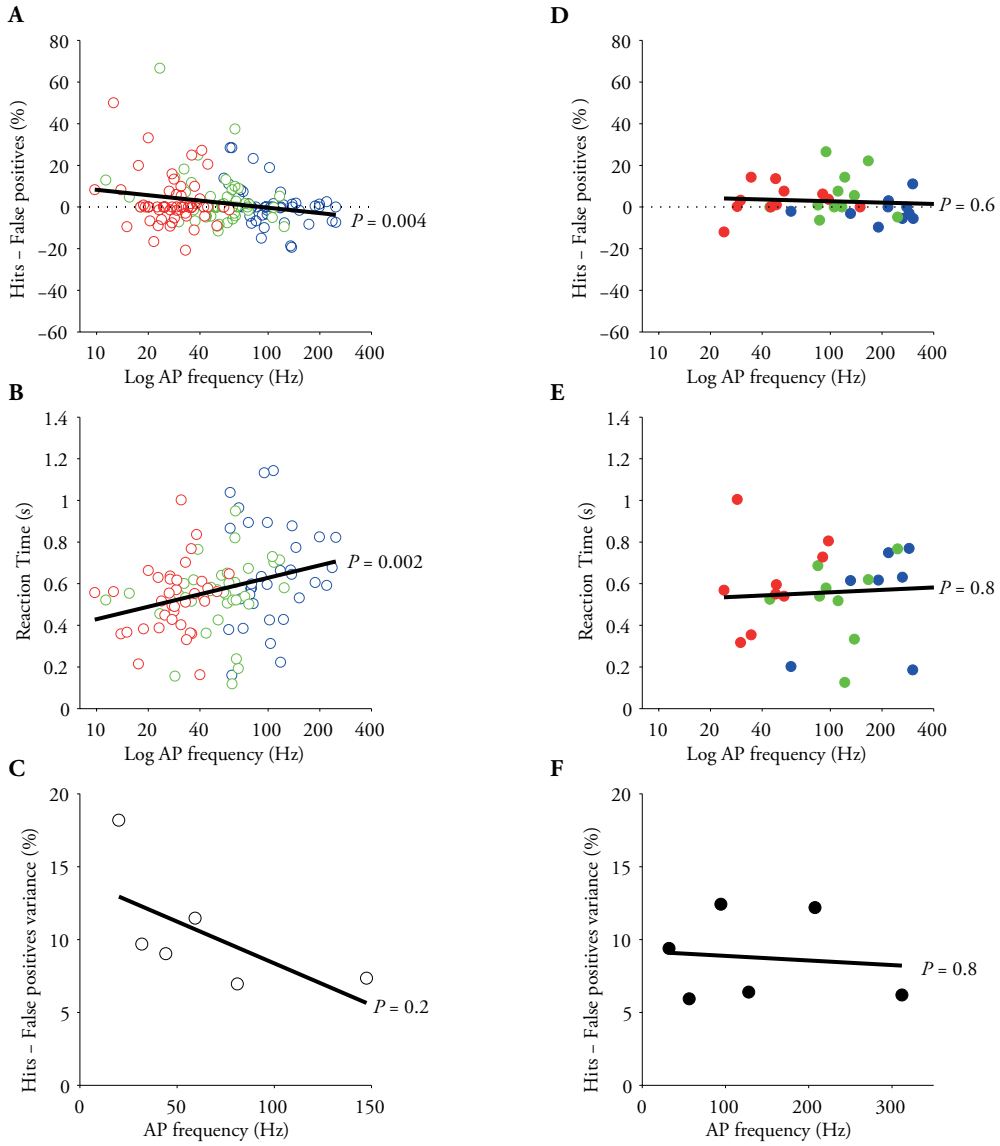

Figure 14: Sensory effect varies with AP frequency in putative excitatory neurons but not in putative inhibitory neurons

(A) Relationship between AP frequency and sensory effects for all conditions within putative excitatory cells (empty circles, n = 55 cells, 3 conditions for each cell, Pearson's R=-0.22). Each data point represents behavioral response to one stimulation condition. Conditions are color labeled according to condition membership (**red**, low frequency stimulation; **green**, medium frequency; **blue**, high frequency). **(B)** Relationship between AP frequency and reaction times for all conditions within putative excitatory cells (R=0.30). Conventions for panels **B, D, E** as in **A**. **(C)** Relationship between AP frequency and standard deviations of sensory effects for all conditions within putative excitatory cells binned into equally sized groups (Pearson's R=-0.64). **(D)** Same as in (A) for putative inhibitory neurons (filled circles, n = 11 cells, 3 conditions for each cell, Pearson's R=-0.09). **(E)** Same as in **B** for putative inhibitory neurons (Pearson's R=0.06, P=0.8). **(F)** Same as in **C** for putative inhibitory neurons (Pearson's R=-0.11, P=0.8).

In order to assess the frequency dependence of effects more rigorously, we performed an across-experiments analysis in which we combined data of several of our current experiments and those of a previously published study [Houweling and Brecht, 2008] (see Table 1). This combined data set included cells exposed to nanostimulation at a variety of stimulation intensities and pulse durations

and which resulted in a variable number and rate of evoked APs. The resulting across-experiments analysis contained a large number of cells (putative excitatory neurons, n=270; putative inhibitory neurons, n=43) stimulated in a large number of trials (putative excitatory neurons, n=16,077; putative inhibitory neurons, n=2,638). Regression analysis showed again that for putative excitatory neurons there was a negative relationship between the detectability of single-cell stimulation and evoked AP frequency (Figure 15A). These negative correlations were also statistically significant for non-logtransformed data (R=-0.20, P=0.01; across-experiments analysis, R=-0.17, P=0.00001). Examining the effect of AP frequency on the consistency of the rat's responses in the across-experiment analysis gave a similar result (Figure 15B). Also, no sensory effects of AP frequency were observed in putative inhibitory interneurons in the across-experiment analysis (Figure 15C, D). Thus, rats reported better low frequency spike trains of putative excitatory neurons compared to medium and high frequency spike trains. In contrast, sensory effects of putative inhibitory neurons were independent of AP frequency in the rat barrel cortex.

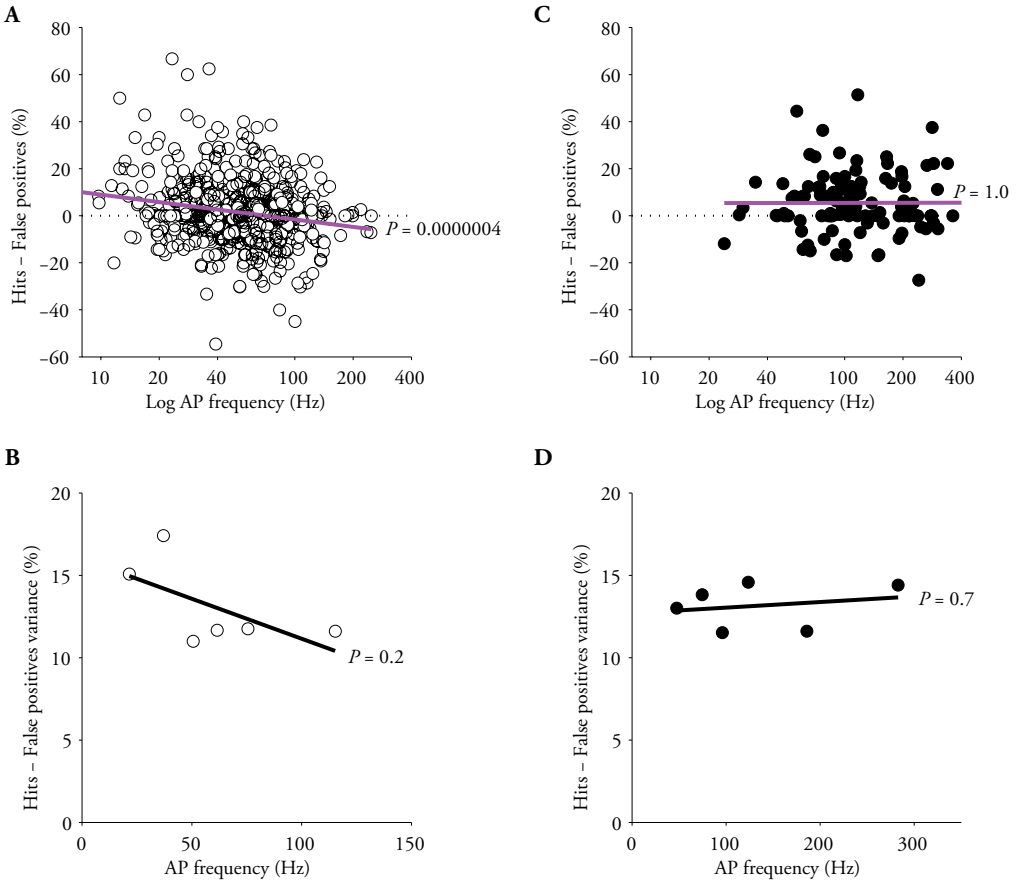

Figure 15: Effects of AP frequency in across-experiments analysis
(A) Relationship between AP frequency and sensory effects for all conditions across putative excitatory cells (n = 270 cells, 3 conditions for each cell, Pearson's R=-0.19). Each data point represents behavioral response to one stimulation condition. **(B)** Relationship between AP frequency and standard deviations of sensory effects for all conditions across putative excitatory cells binned into equally sized groups (Pearson's R=-0.62, P=0.2). **(C)** Same as in **A** for putative inhibitory neurons (filled circles, n = 43 cells, 3 conditions for each cell, Pearson's R=0). **(D)** Same as in **B** for putative inhibitory neurons (Pearson's R=0.22).

5.2.3 AP number only weakly affects detectability but strongly affects response consistency

We wondered how the number of evoked APs in each cell type affects the animal's report. To address this question we performed experiments (n=137 cells) in which we manipulated AP number by applying nanostimulation for 100, 200 and 400 ms at a constant current intensity of on average 6 – 12 nA (which results in comparable AP frequencies across conditions (Figure 9)). Figure 16 shows an example of such an experiment on a putative excitatory neuron. Here, nanostimulation (Figure 16A) evoked on average 5 ± 2 APs during 100 ms current steps (Figure 16B middle), 11 ± 2 APs during 200 ms current steps (Figure 16B 2nd from top) and 24 ± 4 APs during 400 ms current steps (Figure 16B top). Interestingly, the maximal number of lick responses was observed following the short stimulation duration and decreased along with an increase in stimulation duration (Figure 16C). In contrast, the animal responded in all microstimulation trials (Figure 16B bottom), but only once in 41 catch trials

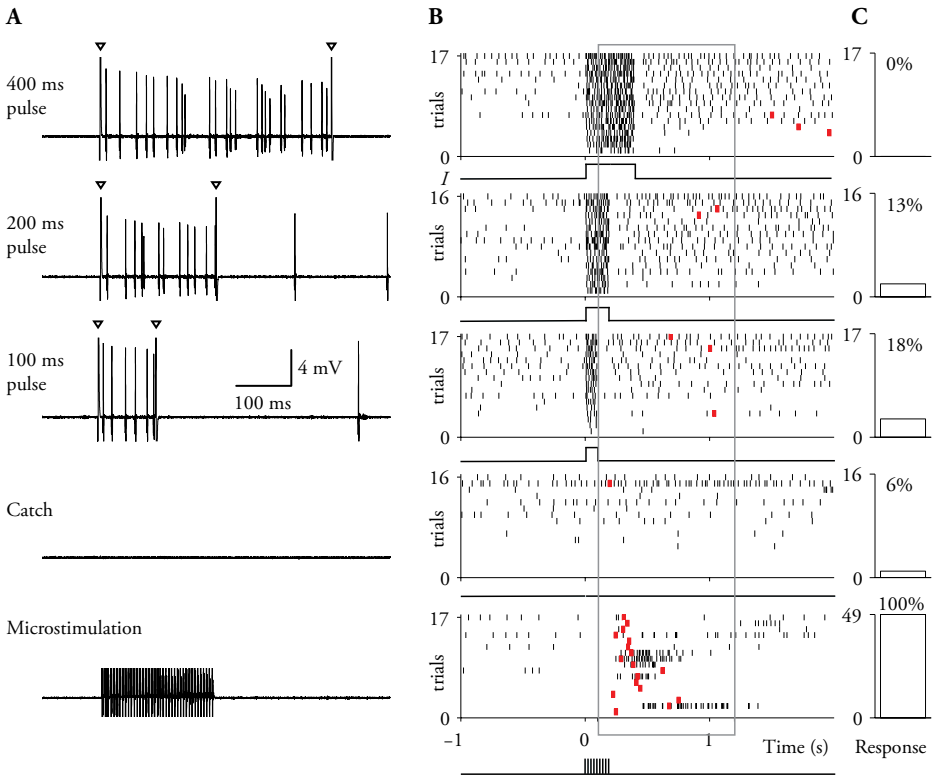

Figure 16: Behavioral responses to stimulation of a putative excitatory neuron with different AP numbers
(A) Single-cell stimulation example traces with juxtacellular current injection of 100 ms, 200 ms, and 400 ms steps, no-current-injection catch trial trace and microstimulation trial trace. Triangles indicate stimulation onset and offset artifacts. In the microstimulation trace artifacts were partially clipped. **(B)** Action potential (ticks) raster plots and first lick responses (red squares) during juxtacellular single-cell stimulation trials conditions, no-current-injection catch trials and 17 randomly selected microstimulation trials (bottom). The neuron was inhibited during and after microstimulation (stimulation current, 3.5 µA). **(C)** Quantification of responses to single-cell stimulation, catch trials and microstimulation.

without stimulation (Figure 16B 4th from top).

The result of a single-cell stimulation experiment in a putative inhibitory neuron is shown in Figure 17. In contrast to putative excitatory neurons, the maximal number of lick responses was observed following the medium and long stimulation durations and was negative for the short stimulation duration.

Due to the limited number of trials in each cell, we assessed the statistical significance of these

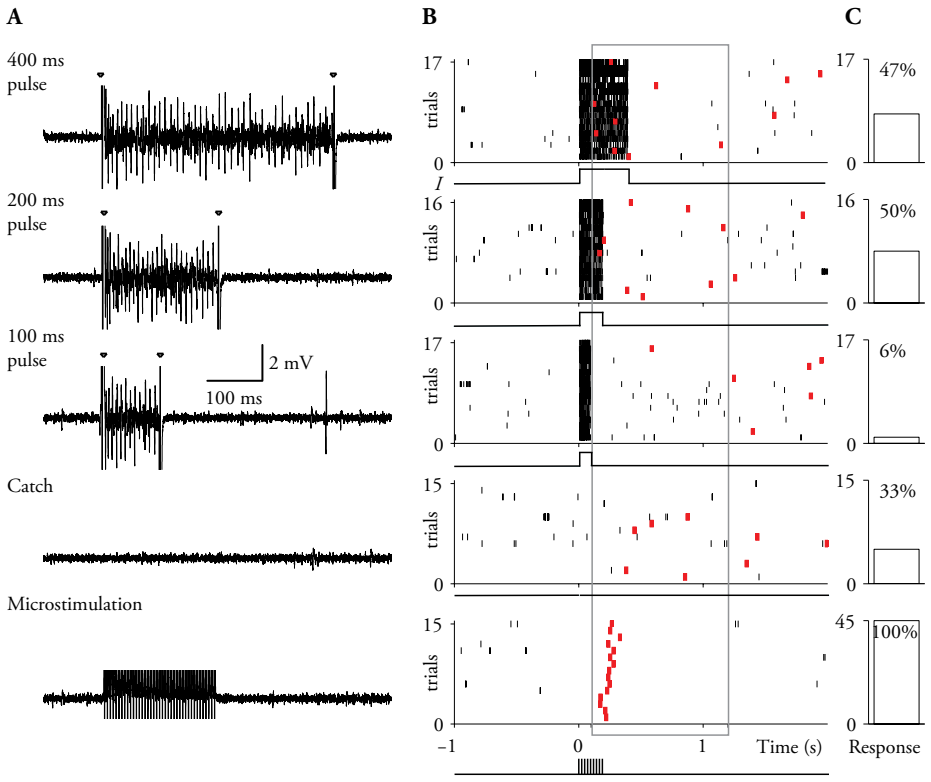

Figure 17: Behavioral responses to stimulation of a putative inhibitory neuron with different AP numbers
(A) Single-cell stimulation example traces by juxtacellular current injection of 100 ms (24 ± 12 APs), 200 ms (39 ± 13 APs), 400 ms (70 ± 36 APs) steps, no-current-injection catch trial trace and microstimulation trial trace. Triangles indicate stimulation onset and offset artifacts. In the microstimulation trace artifacts were partially clipped. **(B)** Action potential (ticks) raster plots and first lick responses (red squares) during juxtacellular single-cell stimulation trials conditions, no-current-injection catch trials and 15 randomly selected microstimulation trials (bottom). The neuron was inhibited during and after microstimulation (stimulation current, 3 μA). **(C)** Quantification of responses to single-cell stimulation, catch trials and microstimulation.

effects over many single-cell stimulation experiments (Figure 18), including a similar set of experiments (n=40 cells) in which we presented nanostimulation currents for 200, 400 and 800 ms. Stimulation frequencies varied to some extent between cells but were similar within cells across all nanostimulation conditions. For putative excitatory cells there was a weak but statistically significant negative correlation between AP number and detectability of single-cell stimulation (Figure 18A). However, no significant

correlation between AP number and reaction time could be observed for putative excitatory cells (Figure 18B). These results were comparable to those obtained with the non-logtransformed data (AP number experiments, R=-0.08, P=0.08; across-experiments analysis, R=-0.09, P=0.01). Interestingly, analyzing the consistency of rats' responses across cells, we observed that for stimulation of putative

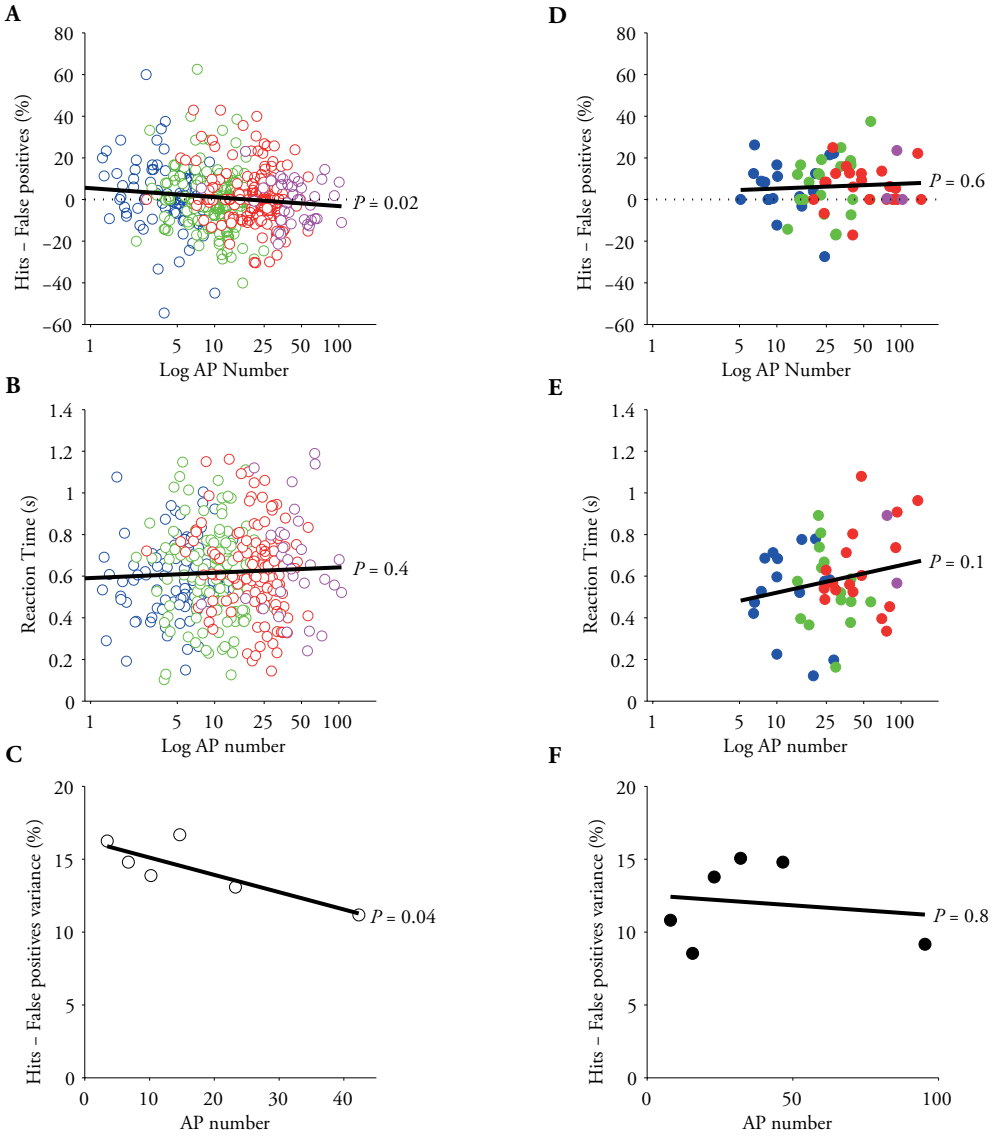

Figure 18: Effect size weakly decreases and response consistency increases with AP number in putative excitatory neurons

(A) Relationship between AP number and sensory effects for all conditions within putative excitatory cells (empty circles, n = 156 cells, 3 conditions for each cell, Pearson's R=-0.11). Each data point represents behavioral response to one stimulation condition. Conditions are color labeled according to condition membership (**red**, 100 ms pulse stimulation; **green**, 200 ms pulse stimulation; **blue**, 400 ms pulse stimulation; magenta, 800 ms pulse stimulation). Conventions for panels **B, D, E** as in **A**. **(B)** Relationship between AP number and sensory effects for all conditions within putative excitatory cells (Pearson's R=0.05). **(C)** Relationship between AP number and standard deviations of sensory effects for all conditions within putative excitatory cells binned into equally sized groups (Pearson's R=-0.82). **(D)** Same as in **A** for putative inhibitory neurons (filled circles, n = 21 cells, 3 conditions for each cell, Pearson's R=0.07). **(E)** Same as in **B** for putative inhibitory neurons (Pearson's R=0.21). **(F)** Same as in **C** for putative inhibitory neurons (Pearson's R=-0.15).

excitatory neurons high AP numbers resulted in a greater consistency of responses across cells (Figure 18C). In addition, no correlation between spike number and effect size or reaction times was observed for putative inhibitory neurons both for the AP number experiments (Figure 18D, E) as well as no response consistency could be reported for these neurons (Figure 18F) .

Examining the effects of AP number stimulation in an across-experiments analysis showed the similar tendencies (Figure 19A ,B). In addition, for putative inhibitory neurons also no correlation between AP number and effect size or response consistency could be reported for these neurons (Figure 19C, D).

We conclude that excitatory neuron detectability weakly but significantly decrease with AP

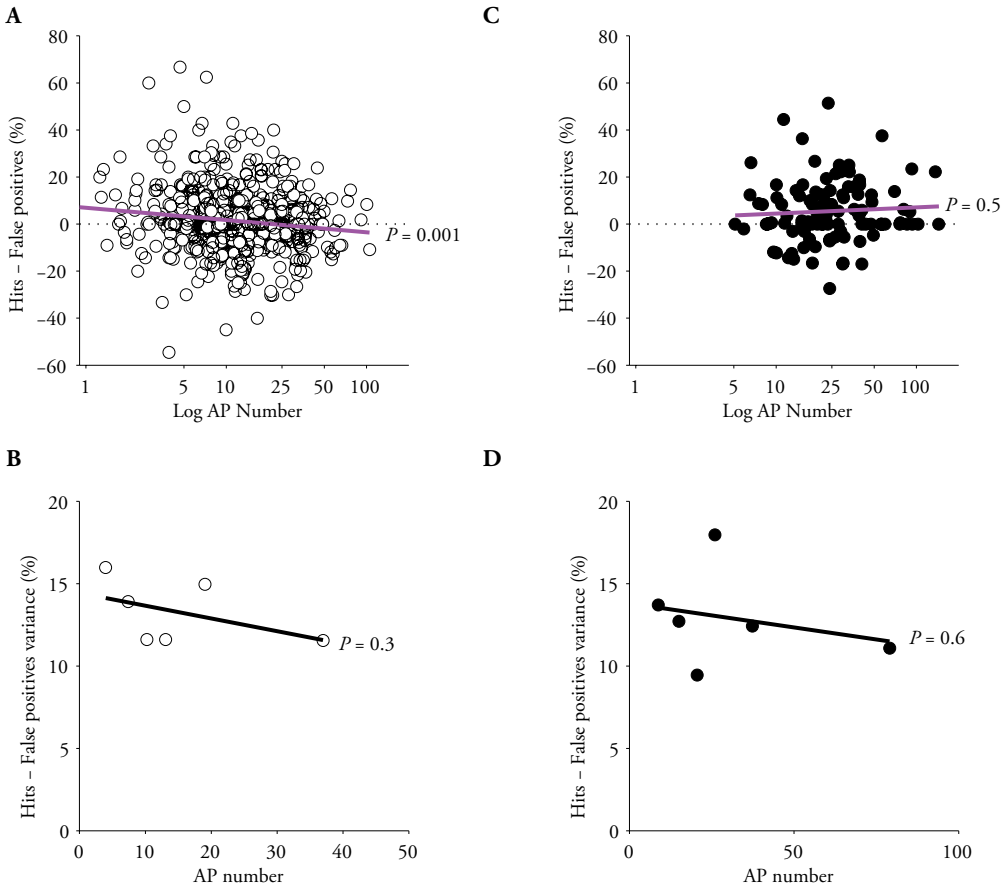

Figure 19: Effects of AP number in across-experiments analysis
(A) Relationship between AP number and sensory effects for all conditions across putative excitatory cells (n = 270 cells, 3 conditions for each cell, Pearson's R=-0.12). Each data point represents behavioral response to one stimulation condition. **(B)** Relationship between AP number and standard deviations of sensory effects for all conditions across putative excitatory cells binned into equally sized groups (Pearson's R=-0.47). **(C)** Same as in **A** for putative inhibitory neurons (filled circles, n = 43 cells, 3 conditions for each cell, Pearson's R=0.06). Conventions are as in **A**. **(D)** Same as in **B** for putative inhibitory neurons (Pearson's R=-0.26).

number. This relationship was not observed in putative inhibitory neurons. The consistency of single-cell stimulation effects across cells strongly increases with AP number.

5.2.4 Single-cell detectability increases with AP irregularity

So far we used simple DC current steps that typically resulted in regular spike discharge patterns. The average bias towards responding evoked under these conditions was small. Since natural spiking patterns in the cortex are highly irregular and contain bursts (Connors and Gutnick, 1990; Gray and McCormick, 1996) we examined how manipulating the regularity of the evoked spike trains affected the animal's responses (Figure 20).

To this end, we stimulated neurons in the barrel cortex using a fluctuating nanostimulation current injection consisting of a combination of step currents with a total duration of 400 ms. The stimulation sequence consisted of 10, 20, 40, 80 and 160 ms step currents with intensities of 100%, 50%, 25%, 12.5% and 6.25%, respectively, along with a negative current pulse of 90 ms duration at 50% current intensity in order to inhibit the cell from firing (Houweling et al., 2010). These step currents were presented in a sequence that was randomized for individual trials (Figure 20A). As a control we induced a regular AP train by using a single 400 ms current step as described before. The irregular stimulation of putative excitatory neurons evoked in most cells a similar AP number (average 9 ± 4 APs) as the regular stimulation condition (11 ± 5 APs). Figure 20 shows an example of such an experiment on a putative excitatory neuron. Most surprisingly, evoking an irregular spiking pattern resulted in a strong positive effect for the irregular AP train stimulation compared to the regular AP train and no-current-stimulation conditions. Lick responses (red squares) occurred more often after the irregular single-neuron stimulation (Figure 20B top) and microstimulation (Figure 20B bottom), but considerably less often after regular single-neuron stimulation (Figure 20B 2nd from top) and no-stimulation catch trials (Figure 20B 3rd from top). Due to the relatively high number of stimulation trials in this recording we could also assess the statistical significance of effect size within the cell (Figure 20C; Fisher's exact test) which suggested that the animal reliably reported irregular single-cell stimulation (P=0.00007) but not regular single-cell stimulation.

The irregularity of the AP train was measured by the coefficient of variation (CV) of the inter-spike interval (ISI) distribution (s.d./mean), and will be referred to as CV_{ISI}. Stimulation of putative excitatory cells with fluctuating currents resulted in spike trains that displayed CV_{ISI} values of 0.95 ± 0.26, which are close to experimentally observed values for natural spike trains. In contrast, single-cell stimulation with regular current steps resulted in much lower CV_{ISI} values of 0.46 ± 0.21. Regression analysis showed a highly significant positive correlation between CV_{ISI} and behavioral effect size (Figure 21A). In addition, a population analysis of 62 putative excitatory cells revealed that evoking irregular spike trains strongly biased animals towards responding (Figure 21B, effect size 7.7%) and to

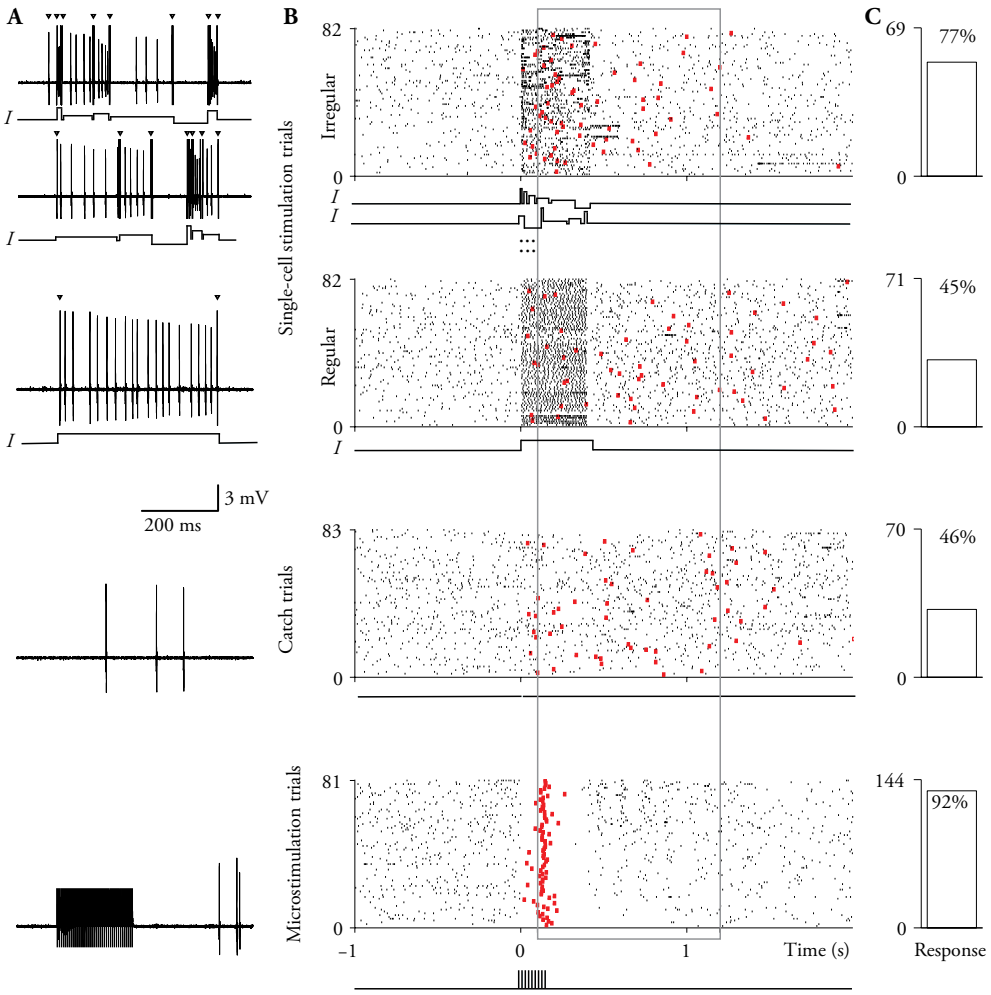

Figure 20: Behavioral responses to regular and irregular spike trains of a single putative excitatory neuron

(A) Two single-cell stimulation example traces by juxtacellular irregular current injection of 400 ms train (top and 2nd from top, 18 ± 6 APs) composed of 5 current steps of 10, 20, 40, 80 and 160 ms at current intensities of 100, 50, 25, 12.5 and 6.25 % of maximal intensity, respectively, and in addition 90 ms negative pulse at 50 % of maximal intensity. Current steps order was randomized across trials. As control were used juxtacellular regular current step of 400ms (middle, 13 ± 6 APs), no current injection trial (4th from top) and microstimulation trial trace (bottom). Triangles indicate stimulation onset and offset artifacts. In the microstimulation trace artifacts were partially clipped. **(B)** Action potential (ticks) raster plots and first lick responses (red squares) during irregular and regular juxtacellular single-cell stimulation trials conditions, no-current-injection catch trials and 83 randomly selected microstimulation trials (bottom). The neuron was inhibited during and shortly after microstimulation (stimulation current, 4 μA). **(C)** Quantification of responses to single-cell stimulation, catch trials and microstimulation.

a statistically significant (Figure 21C) larger degree than regular spike trains (Figure 21A-C).

However, the consistency of behavioral responses between cells was similar across CV_{ISI} values (R=-0.15, P=0.8). Furthermore, no correlation between CV_{ISI} and behavioral reaction times was found for these cells (R=-0.02; P=0.9). A population analysis of 12 putative inhibitory neurons revealed similar trend (Figure 21D). Also, stimulating putative inhibitory neurons with irregular spike trains biased rats towards responding (Figure 21E, effect size 9.9%) and to a statistically significant (Figure

21F) larger degree than regular spike trains (Figure 21E, F, effect size -0.4%).

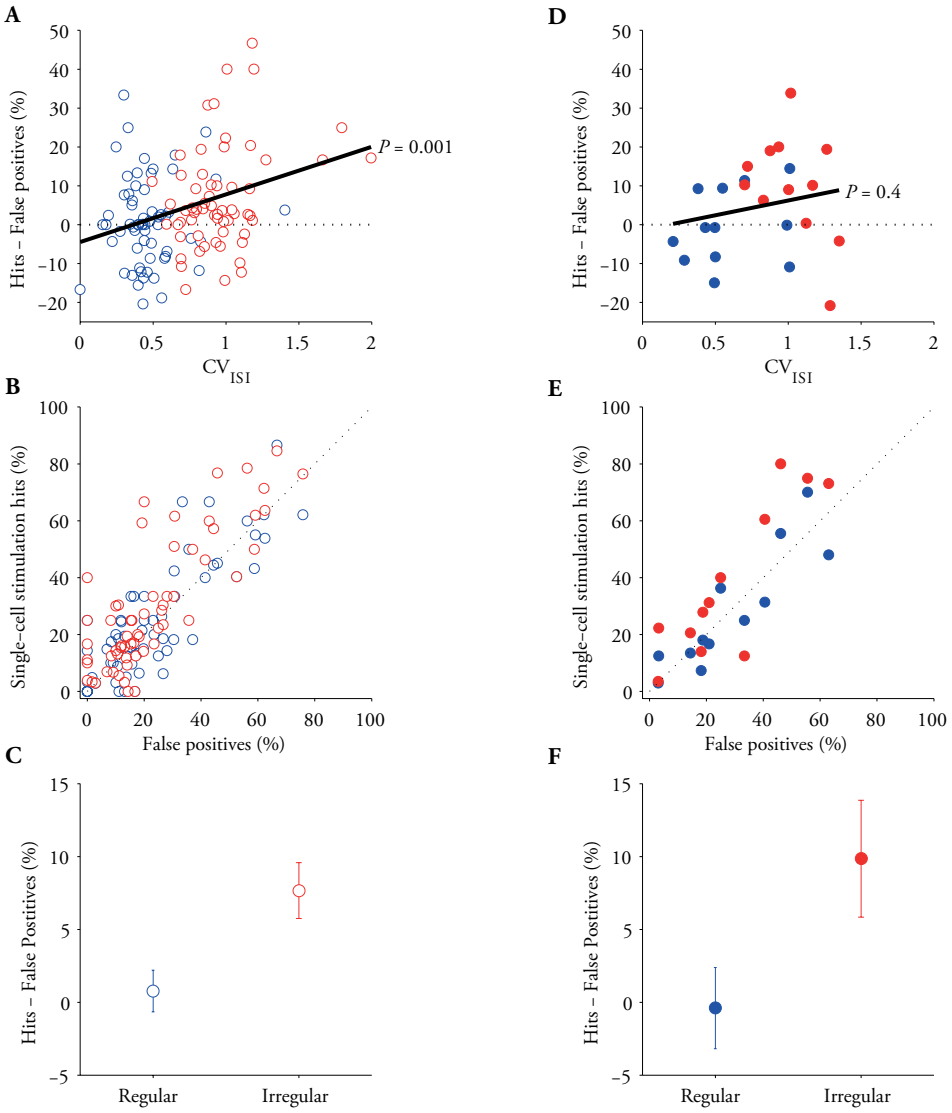

Figure 21: Initiation of irregular AP trains in putative excitatory and inhibitory neurons strongly biases towards responding

(A) Relationship between AP number and sensory effects for all conditions within putative excitatory cells (empty circles, n = 62 cells, 2 conditions for each cell, Pearson's R=0.31). Each data point represents behavioral response to one stimulation condition. Conditions are color labeled according to condition membership (**blue**, 400 ms pulse regular stimulation; **red**, 400 ms pulse irregular stimulation). Conventions for panels **B-F** as in **A**. **(B)** Response rates for single-cell stimulation trials (hits) versus no-current-injection catch trials (false positives) of putative excitatory neurons. one-sided paired t-test; Regular stimulation, P=0.3; Irregular stimulation, P=0.00009. **(C)** Comparison of sensory effects (single-cell stimulation hit rate - catch trial response rate) of regular and irregular single-cell stimulations. two-sided paired t-test, P=0.0001. **(D)** Same as in **A** but for putative inhibitory neurons (filled circles, n = 12, R=0.27; P=0.4). **(E)** Same as in **B** but for putative inhibitory neurons. one-sided paired t-test; Regular stimulation, P=0.6; Irregular stimulation, P=0.02; **(F)** Same as in **C** but for putative inhibitory neurons. two-sided paired t-test, P=0.01.

Our findings on the effects of AP regularity were supported by an across-experiments meta-

analysis, in which we calculated CV_{ISI} for the spike trains evoked with simple current steps. Here we also observed stronger sensory effects for larger CV_{ISI} values (data not shown). Altogether, these findings indicate that other coding schemes might be involved in sensory stimulation of barrel cortex neurons. One such possible form of neural code can be brief bursts (Lisman, 1997), which is probably an extreme case of irregular firing pattern. Furthermore, bursts can trigger dendritic spikes and influence dendritic integration properties (Larkum et al., 1999). Therefore, we wondered whether inducing very few spikes in a short current step followed by a long inhibition period would result in a response bias in both cell types (Figure 22).

To this end, we stimulated inhibitory and putative excitatory neurons in the barrel cortex using short current step of 25 ms and inducing 1-3 APs (putative excitatory neurons; 2.6 ± 0.2 APs; putative inhibitory neurons; 2.97 ± 0.41 APs), resulting in average firing rates of 105 Hz and 120 Hz for putative excitatory and inhibitory cells, respectively. Importantly, in order to avoid the possible effect of after discharge to prevent any further spiking activity following nanostimulation (Figure 7) we inhibited the cell from firing until the end of the trial by injecting negative current (50% of current intensity used for nanostimulation) following the brief stimulation current step. Figure 22A-C shows an example of such an experiment on a putative excitatory neuron. Most surprisingly, 1-3 evoked APs resulted in a strong positive effect for the short current step high frequency stimulation compared to no-current condition. Specifically, nanostimulation stimulation (see Figure 22A for example trace) evoked on average 2.03 APs at a frequency of 80 Hz and a CV_{ISI} value of 2.6 (compared to CV_{ISI} value of 1.0 for no-current-stimulation catch trials during the same time window; two-sided independent samples t-test, $P < 0.01$). Lick responses (red squares) occurred more often after the single-cell stimulation (Figure 22 top) and microstimulation (Figure 22B bottom), but considerably fewer times after no stimulation catch trials (Figure 22B middle). Quantification of responses (Figure 22C, see methods) suggested that the animal reported single pyramidal cell activity. A population analysis of 30 putative excitatory cells revealed that inducing 1-3 spikes biased the animal towards responding (Figure 22D; n=30 cells; effect size: 6.3%; Student's paired t-test, P=0.02, red filled circle denotes example cell in Figure 22A-C). In contrast, inducing similar spike number in 11 inhibitory cells failed to show a similar effect (Figure 22E; effect size: -2.4%; P=0.7). Importantly, comparing irregularity of the evoked brief stimulation trials (including inhibition period) over 2 s from the start of stimulation (CV_{ISI} = 2.24) to that of the evoked no-current-injection stimulation trials over the same period of time (CV_{ISI} = 0.86) was highly significant across all trials ($P < 0.00000000001$). In conclusion, these findings suggest that rats are extremely sensitive to the temporal structure of the sensory input, which contains more information in the relation of the spikes' timing than in the sheer number of spikes.

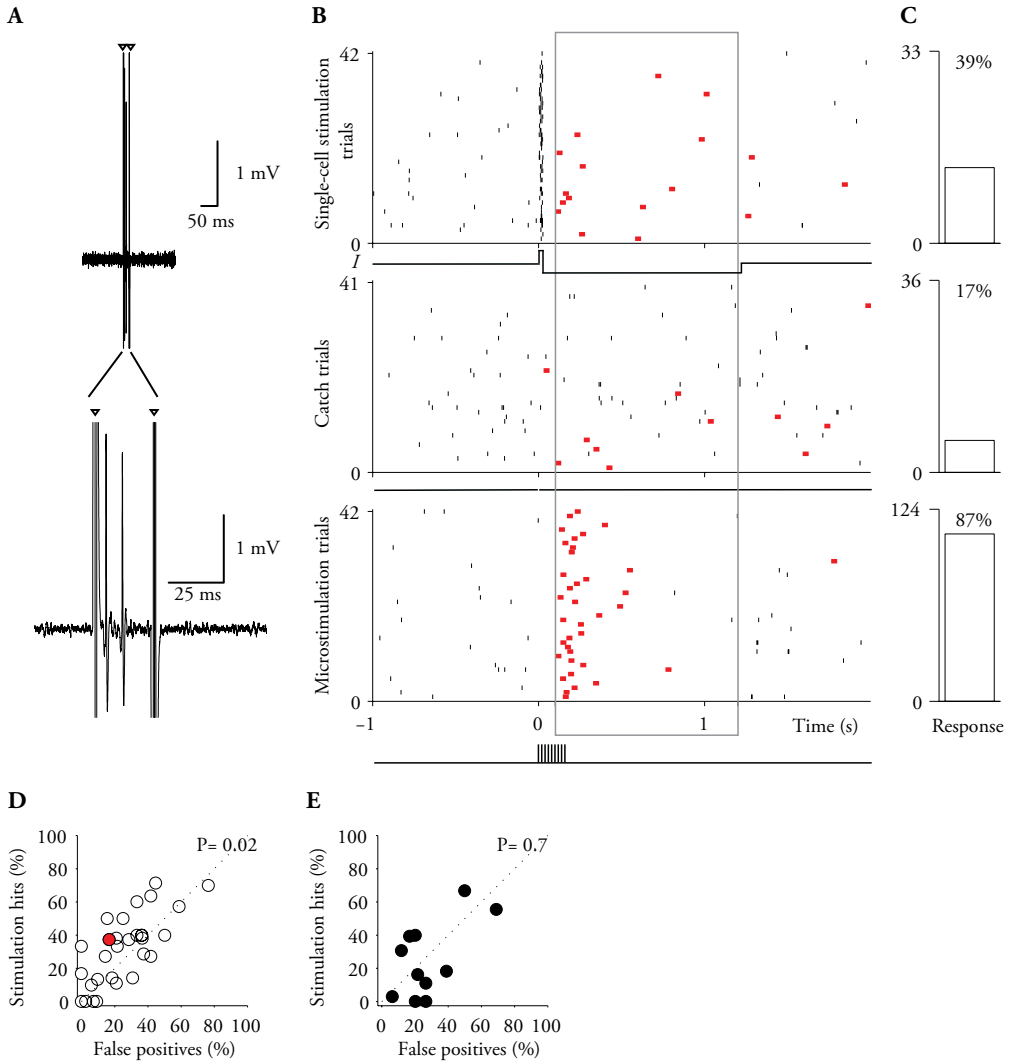

Figure 22: Initiation of burst-like AP train in putative excitatory neurons but not inhibitory neurons biases towards responding

(A) Single-cell stimulation example traces by juxtacellular current injection of 25 ms step (top) and enlarged view of the same trace (bottom). Triangles indicate stimulation onset and offset artefacts. **(B)** Action potential (ticks) raster plots and first lick responses (red squares) during juxtacellular single-cell stimulation trials condition, no-current-injection catch trials and 42 randomly selected microstimulation trials (bottom). The neuron was inhibited during and after microstimulation (stimulation current, 5 μA). **(C)** Quantification of responses to single-cell stimulation, catch trials and microstimulation. **(D)** Response rates for single-cell stimulation trials (hits) versus no-current-injection catch trials (false positives) of minimal evoked APs in putative excitatory neurons (n=30 neurons; mean hit rate 32.1%; mean false-positive rate 25.8%; note several points coincide). Red filled circle mark example cell (panels **A-C**). **(E)** Response rates for single-cell stimulation trials (hits) versus no-current-injection catch trials (false positives) of minimal evoked APs in putative inhibitory neurons (n=11 neurons; mean hit rate 25.5%; mean false-positive rate 27.9%; note several points coincide).

5.2.5 State dependence of single-cell stimulation detectability

Previous studies in humans showed that ongoing brain states can influence conscious perception (Linkenkaer-Hansen et al., 2004; Jones et al., 2007; Schubert et al., 2009). In addition, a recent

single-cell stimulation study in mice demonstrated the effect of single-neuron activity on brain states (Li et al., 2009). We therefore wondered whether behavioral responses to single-neuron stimulation were state-dependent. To this end we examined the relationship between prestimulus neuronal local field potential (LFP) and single-neuron stimulation detectability. We found that hits (correct responses on nanostimulation trials) were preceded by an increased power in frequency range of 12 - 18 Hz compared to misses (Figure 23A, paired t-test, P=0.04) as predicted by human studies (Linkenkaer-Hansen et al., 2004; Jones et al., 2007; Schubert et al., 2009) but not across the entire examined range of 4 to 30 Hz (P=0.3). Interestingly, for the catch trials without stimulation we noticed that correct rejections were preceded by significant increased power in the frequency range of 4 – 30 Hz compared to false positives (Figure 23B, paired t-test, P=0.03) and specifically higher in the selected frequency range (12 – 18 Hz, P=0.01). Thus, behavioral responses to single-cell stimulation were state-dependent in a manner such that increased power in this frequency range predicted correct responses.

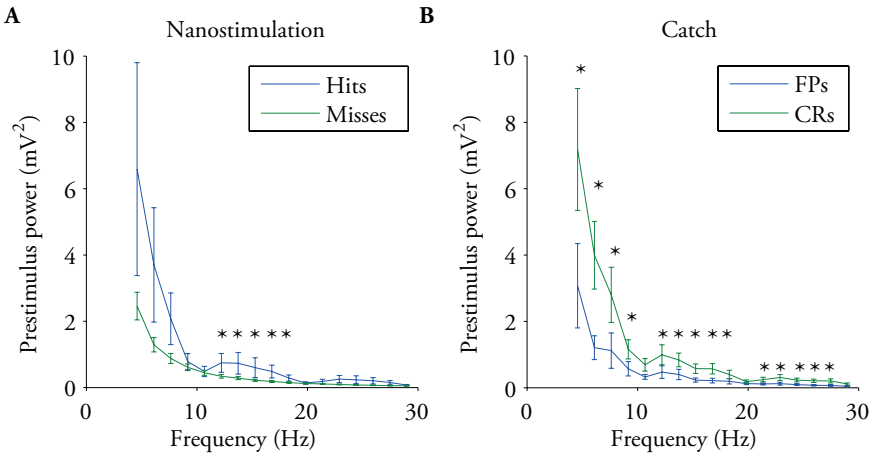

Figure 23: Increase in low frequencies oscillation power predicts single-neuron stimulation hits

(A) Relation between prestimulus LFP frequency and power for average single-cell stimulation hits (blue line) and single-cell stimulation misses (green line). mean ± s.d. two-sided paired t-test for all range (4 – 30 Hz) P=0.2. * two-sided paired t-test for selected range of 12 – 18 Hz, P=0.04. **(B)** Relation between prestimulus LFP frequency and power for average catch trials false positives (FPs, blue line) and catch trials correct rejections (CRs, green line). mean ± s.d. two-sided paired t-test for all range (4 – 30 Hz) P=0.03. * two-sided paired t-test for selected range of 12 – 18 Hz, P=0.01.

6. Discussion

In this study we aimed to examine the effect of spiking parameters on the detectability of single-neuron stimulation in excitatory and inhibitory neurons of the rat barrel cortex. In order to do so we first needed to develop a technique which allows parametric manipulation of AP frequency, AP number and AP regularity. In the first part of this work we provided a detailed description of nanostimulation, a novel technique which permits manipulation of single neuron activity by juxtacellular current injection. We described the properties of this technique and demonstrated that nanostimulation can be directed to a variety of identifiable neurons in anesthetized and awake animals. Most importantly we showed that nanostimulation allows control of AP frequency and AP number. Furthermore, we demonstrated that this technique can be used to selectively inhibit sensory responses in identifiable neurons, thus inducing irregular AP trains in the stimulated neuron.

6.1 Nanostimulation stimulates a single neuron and induces cell-specific effects

A key aspect of both juxtacellular labelling and nanostimulation is that these procedures target single neurons. The evidence for this idea has been reviewed in depth before (Pinault, 1994, 1996; Herfst and Brecht, 2008; Voigt et al., 2008). Briefly, the argument is as follows: (i) Nanostimulation currents (3-30 nA) are about 2-3 orders of magnitude smaller than those thought to be required for activating neurons with microstimulation (> 1 μA) (Stoney et al., 1968). In line with these small currents the biophysical considerations above suggest that nanostimulation acts in the micrometer range below the electrode tip. (ii) Inadvertent stimulation of a second nearby neuron, detected by the presence of large additional AP waveforms, is a rare event (< 1% of APs) (Houweling and Brecht, 2008; Voigt et al., 2008). This is consistent with the low probability that two neurons are in close contact with a 1-2 μm tip. (iii) Cells more distant from the pipette than the primary neuron targeted for nanostimulation, detected by the presence of small additional AP waveforms (< 0.5 mV) in the recording, are not affected in their activity (Houweling and Brecht, 2008; Voigt et al., 2008). (iv) Histological data confirm a one-to-one correspondence between single juxtacellularly activated and labelled neurons (Pinault, 1994, 1996). Furthermore, electric destruction of single juxtacellularly labelled neurons results in the histological recovery of single cells with disintegrated morphologies (Pinault, 1994).

In line with these methodological considerations we found that nanostimulation effects were highly cell-specific. For example, whisker movements evoked by single-cell stimulation in the facial nucleus were completely contingent on spiking of the respective neurons (without any movement failures) (Herfst and Brecht, 2008). Furthermore, whisker movements varied with respect to direction,

amplitude and speed as a function of the identity of the stimulated neuron.

6.2 Properties of nanostimulation

The effects of the juxtacellular current injections used for nanostimulation are in many ways similar to those of intracellular current injections. First and foremost, neurons are excited by positive currents (Figure 8, Figure 9) and inhibited by negative currents (Figure 10). Even more importantly in this research context, nanostimulation current-AP-frequency curves are close to linear for cortical neurons (Figure 8, Figure 9), as described for intracellular recordings (Creutzfeldt, 1995; Nowak et al., 2003). This feature allows a direct manipulation of AP frequency, by combining decreased current intensities with increased current duration, resulting in similar AP numbers over different durations and thus different AP frequencies. Post hoc analysis of the AP frequency experiment (Figure 14) provide evidence that such manipulation successfully managed to do so (Figure 24A). In a similar

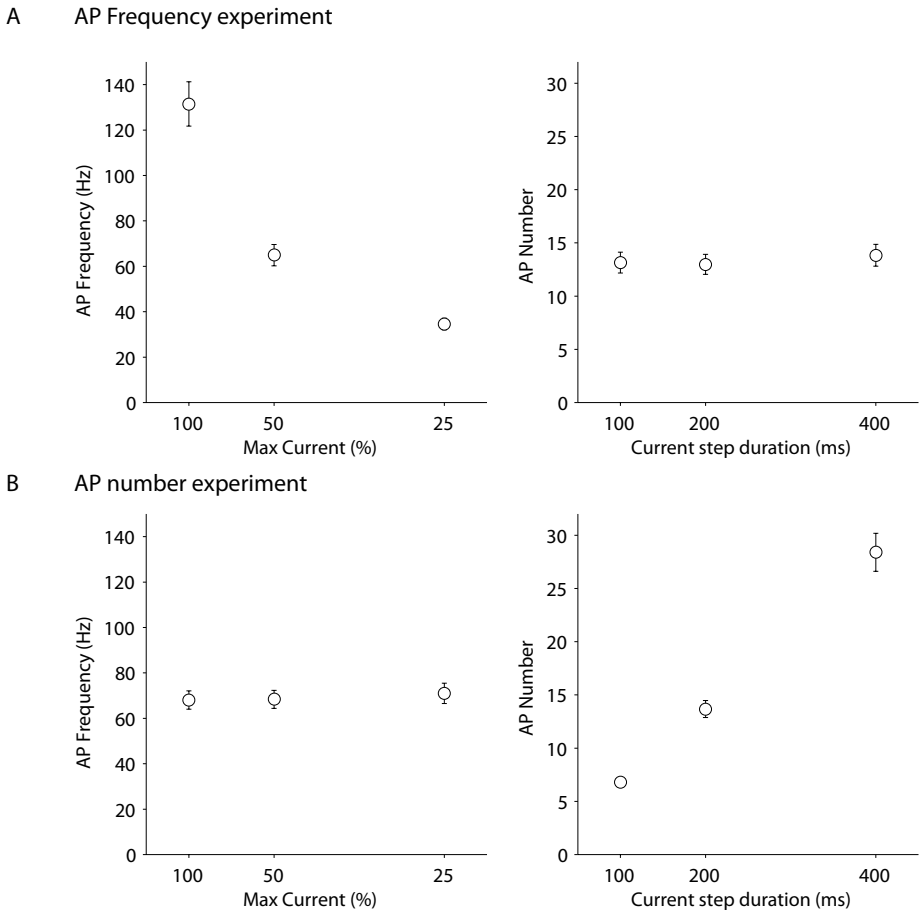

Figure 24: AP frequency and AP number control using nanostimulation
(A) Left panel, Average AP frequency varied linearly with stimulus intensity using different durations of 100 ms (max. current), 200 ms (50 % of max. current) and 400 ms (25 % of max. current). Right panel, AP number was similar across conditions. **(B)** Left panel, Average AP frequency remained stable across different current step durations. Right panel, AP number varied linearly with current step duration.

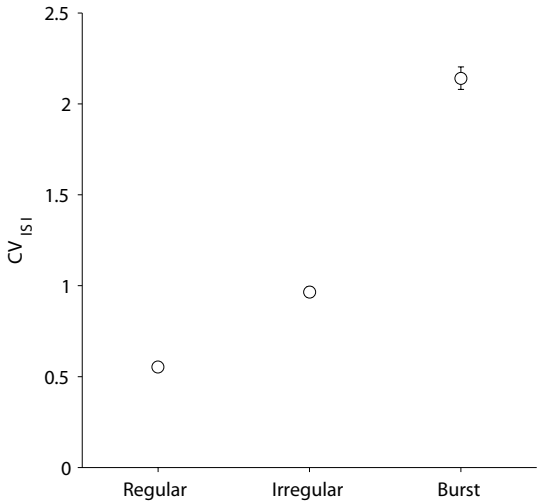

Figure 25: CV_{ISI} average for different stimulation conditions
Average CV_{ISI} increased across different current step conditions. **Regular**: current step duration of 400 ms, **Irregular**: several current steps of a total duration of 400 ms, **Burst:** brief pulse of 25 ms duration followed by long inhibition of about 1.2 s.

fashion, increasing current durations without changing current intensities (Figure 18) resulted in AP number manipulation with constant AP frequencies (Figure 24B). Moreover, combining several current steps of different frequencies in addition to negative current, led to highly irregular AP trains compared with a single component current step (Figure 25). Notably, sustained DC current injections result in AP responses with large temporal jitter (Figure 7), much like AP responses elicited by DC current injections in the whole-cell configuration (Mainen and Sejnowski, 1995). In addition, most cells do not fire instantaneously upon current onset. This may be explained as capacitive charging of the neuronal membrane, which also delays AP initiation upon intracellular current injection. Different from intracellular current injections, nanostimulation may induce in some neurons a small increase in spontaneous AP firing following the injection, a phenomenon might be related to membrane resealing processes.

6.3 Neural coding in excitatory and inhibitory neurons

The successful application of nanostimulation prompted us to investigate the potential contribution of different spiking parameters in behavioral response to single-neuron stimulation during a sensory detection task. In order to better elucidate the role of specific cell populations in single-cell stimulation we examined separately AP frequency and number in putative excitatory and inhibitory interneurons. We find that fast-spiking putative interneurons are more detectable (Figure 11) as we previously reported (Houweling and Brecht, 2008). It may also be the case that interneuron effects depend less critical on spike frequency (Figure 13) and number (Figure 17) but this issue needs further investigation. In line with a powerful effect of interneuron activity on network activity a previous study in hippocamal slices indicated that such GABAergic interneurons may function as hubs and trigger population synchronization (Bonifazi et al., 2009). Further evidence for the role of putative interneurons in synchronous activity comes from a study of FS interneurons in somatosensory barrel cortex of awake rabbits (Swadlow, 2003). Importantly, FS neurons are highly connected via both GABAergic chemical and electrical synapses (Galarreta and Hestrin, 1999, 2002; Gibson et al., 1999) which further support the ability of single interneurons to initiate activity in neural circuits (Cardin

et al., 2009). While the initial neuronal response to microstimulation varies under our conditions (Houweling and Brecht, 2008), we usually observe a long lasting inhibition after the microstimulation train. We therefore wonder if we trained the animal in our microstimulation detection task to report this neuronal inhibition. This hypothesis might explain why animals report so readily inhibitory-cell activity and increasing AP frequency leads to progressively increasing biases away from responding. A recent study reported that in-vivo low frequency optogenetic stimulation (Zhang et al., 2007) of excitatory layer 2/3 neurons in the barrel cortex results in a state-dependent recruitment of inhibitory neurons, with FS neurons being most active and firing the largest number of APs (Mateo et al., 2011). Furthermore, other studies showed that activity of a single pyramidal cell may be sufficient to induce such inhibition (Kapfer et al., 2007), presumably via recruitment of somatostatin-expressing inhibitory interneurons (Silberberg and Markram, 2007).

6.4 Effect of action potential frequency and number in putative excitatory neurons

We find that AP frequency is a critical parameter in detection of single-cell stimulation of excitatory neurons in the rat's barrel cortex. A previous study in the rat motor cortex provided evidence for influence of single pyramidal cells on whisker movement in AP frequency dependent manner (Brecht et al., 2004). The authors reported that increased frequency resulted in the larger amplitude whisking movements whereas the lowest frequency caused whisker movement in the opposite direction. Interestingly, we found that stimulating single somatosensory cortical cells with low frequency stimulation had the biggest sensory effect whereas high frequency stimulation had an opposite effect (Figure 12, Figure 14, Figure 15). Similar to the present findings it was observed that detectability of microstimulation in the barrel cortex of awake head retrained rats decreased with pulse frequency and that even a bias away from reporting was induced by high frequency trains (Butovas and Schwarz, 2007). However, the animals were able to detect an increase in AP frequency more consistently, as reflected by decreased variance with increased AP frequency (Figure 14). Thus, a wide range of findings provide convergent evidence for the idea that cortical signaling is highly frequency dependent.

Surprisingly, evoking a few spikes in putative excitatory neurons had a larger sensory effect compared with initiation of many spikes in the same cells (Figure 16, Figure 18, Figure 19). This observation deviates from a previous report which concluded that monkeys use a simple accumulative counting strategy in S1 for vibrotactile discrimination (Luna et al., 2005). Remarkably, rats did report the increasing numbers of APs with better consistency across cells (Figure 18).

6.5 Significance of irregular neural coding in excitatory and inhibitory neurons

Several models suggested a key role of spiking irregularity in cortical information processing (Abeles et al., 1993; Softky and Koch, 1993; Mainen and Sejnowski, 1995; Bair and Koch, 1996) while others considered it as noise in the system (Shadlen and Newsome, 1994, 1998). In order to examine directly the possible role of irregularity in behavioral detection of single-neuron stimulation we elicited irregular spike trains in both putative excitatory and inhibitory neurons and compared it to regular spike trains with approximately similar evoked AP number (Figure 20). Much to our surprise we found a behavioral effect approximately twice bigger than previous observations (Houweling and Brecht, 2008). In addition, the two stimulation conditions in this experiment could be nicely separated according to the CV_{ISI}. However, no correlation between CV_{ISI} and effect size consistency was found in both cell types. Importantly, examination of the previous experiments revealed similar tendency of the rats to report irregular trials compared with more regular ones but only for excitatory neurons and not for inhibitory neurons (data not shown). Notably, when we stimulated putative interneurons with a short and highly irregular burst-like high frequency stimulation of few spikes only, the rats failed to respond to it (Figure 22). In contrast, evoking a short burst-like activity in excitatory neurons resulted in a strong sensory effect. A possible explanation for such a positive effect in excitatory neurons may lie in the temporal form of this stimulation. Other studies which examined sensory processing in the weakly electric fish also report that pyramidal neurons encode more features than isolated spikes and carry more useful information in the form of bursts (Gabbiani et al., 1996; Metzner et al., 1998; Oswald et al., 2004). A simple leaky integrator model was proposed to account for the role of bursts in a sensory detection task in this species (Goense et al., 2003). In addition, a recent study also suggests a behavioral role for sensory bursts in auditory interneurons of crickets (Marsat and Pollack, 2006). Several other studies also stressed the significance of AP bursts as elementary information units (Cattaneo et al., 1981; Crick, 1984; Otto et al., 1991; Bair et al., 1994; Lewicki and Konishi, 1995; Livingstone et al., 1996; Lesica and Stanley, 2004). Interestingly, application of high-frequency doublets of microstimulation at near threshold levels in the rat barrel cortex also resulted in the highest perceptual efficacy (Butovas and Schwarz, 2007). Thus, it may be possible that rats can detect and respond to initiation of single bursts events in stimulation of single cortical putative excitatory neurons, which does not seem to be the case for putative inhibitory neurons.

What could be the source of the experienced neuronal irregularity that would lead the rat to readily detect it? A possible explanation may be related to the properties of the network activity which provide input to that neuron. Several model studies have shown that networks of excitatory and

inhibitory neurons with definite random connectivity can produce highly irregular spiking activity (van Vreeswijk and Sompolinsky, 1996; Kistler and De Zeeuw, 2002) and fast global oscillations (Brunel and Hakim, 1999).

Interestingly, a recent study examined the neuronal responses in rat barrel cortex to trains of whisker movements at different frequencies with either a periodic or an irregular, "noisy" temporal structure (Lak et al., 2008). The researchers reported that stimulating whiskers above 10 Hz using temporal noise trains led to a larger response magnitude and sharpening of the temporal precision of response to the individual deflections of the stimulus train, suggesting that neurons are tuned to respond differently to temporal unpredictability. The fact that neural firing is highly irregular in the awake behaving brain (Softky and Koch, 1993) in addition to our finding of increased detectability of temporally irregular stimuli makes us speculate that perhaps the perceptual impact is maximized with irregular input and that neurons communicate with each other more efficiently this way.

6.6 Summary and future directions

In summary, our data suggest that complex read-out mechanisms translate single-cell activity into sensory effects in rat somatosensory cortex. In agreement with a recent study, which examined several possible neural code models, the effects of individual spikes do not simply add as suggested by decoding scheme in which the animal counts spikes (Jacobs et al., 2009). Instead we find in our detection task that the sign and the amplitude of sensory effect are determined by AP frequency. AP number in contrast has only a minor effect on the sign and the size of sensory effect, but it strongly affects the consistency of the sensory effect across cells. Finally, spike regularity strongly affects the effect size with the animal weighing irregular spike trains more heavily than regular ones. The fact that the rat reacts even to very brief spike trains further demonstrates that awake attentive animals can be extremely sensitive to cortical action potentials. Thus, our data enforce the view that – given the right parameters – single neuron activity can have a substantial impact on behavior.

6.6.1 Impact of single-neuron stimulation on neuronal populations

Further assessment of the behavioral effect of single-neuron stimulation will be greatly aided by examination of neuronal population response to such perturbation. One possible approach can be implemented by imaging of distinct neuronal population in-vivo while stimulating single neurons with different parameters. A recent study by Kwan and Dan (2012) took the first step in this direction by examining excitatory and inhibitory activity using two-photon calcium imaging along with targeted patching and stimulation of single pyramidal neurons in the rat visual cortex. Interestingly

they reported that burst spiking of more than 5 spikes in single pyramidal neuron selectively activated non-fast spiking somatostatin expressing interneurons but not fast-spiking parvoalbumin expressing inhibitory neurons, which were more correlated with local network activity. The authors thus suggested distinct roles for two major inhibitory circuits; one detecting spike bursts while the other reflecting distributed network activities (Kwan and Dan, 2012). Similarly, such a technique can be used in order to examine the microcircuit which underlies detectability of single-neuron activity and the role of specific neuronal subpopulations in this process. A complementary approach to assess the number and identity of cells which participate in this behavior is implemented by using of the recently developed method of automated ex-vivo serial two-photon tomography (Ragan et al., 2012). This state-of-the-art technique allows quantification of neuronal activity, taking advantage of mice line expressing neuronal markers as the immediate early gene c-fos. Thus, mice can be trained in single-neuron detection task and later on subjected for further analysis of c-fos expression in the barrel cortex and other related brain areas following this procedure. Such analysis can lead to further insights regarding the identity and spatial location of candidate neurons in this neuronal circuit. Yet, another novel imaging technique applied fast two-photon in vivo imaging with three-dimensional random-access scanning in order to visualize calcium activity in hundreds of neurons simultaneously (Katona et al., 2012). Thus, it may be possible in the future to perform single-neuron stimulation experiments under a two photon microscope and register neuronal activity of sensory information processing in the awake behaving brain.

6.6.2 Reconstruction of neuronal connectivity of single-neuron activity

Another application which can substantially advance our understanding of the role of single neurons in neural circuit is via single-cell genetic manipulation. Such an application that bridges physiology and genetics was recently developed using viral transfection of single neurons via whole-cell recordings (Rancz et al., 2011). The authors demonstrated for the first time the ability to record from single neurons and then deliver DNA plasmids that allowed retrograde, monosynaptic tracing of each neuron's presynaptic inputs. Potentially, such a technique can be applied also to our task. Importantly, whole cell recordings in awake behaving animals are difficult to obtain and limited in their stability over time. Nevertheless, obtaining such recording in addition to stimulation of the recorded neuron can reveal the functional connectivity of specific local and long-range networks of the manipulated cell.

6.6.3 Manipulation of single-cell activity using optogenetics

Optogenetics techniques allow control of neuronal activity in specific neuronal subpopulations

(Boyden et al., 2005; Gunaydin et al., 2010). However, the temporal and spatial activation of single cells is still challenging (Schoenenberger et al., 2008; Rickgauer and Tank, 2009). A recent technique termed temporally focused laser pulses (TEFO) demonstrated the possible optogentic activation of single-neurons in hippocampal slices (Andrasfalvy et al., 2010). A different approach to the same problem was adopted by LeChasseur et al. (2011) who developed dual-core fiberoptics–based microprobes, with an optical core to locally excite and collect fluorescence, and an electrolyte-filled hollow core for extracellular single unit electrophysiology. The researchers demonstrated the use of this method in anesthetized mice, by combining detection and activation of single channelrhodopsin-expressing neurons. Thus, the application of such optogentetically derive methods can be potentially combined with in-vivo awake recordings and stimulation of single-neurons in a behavioral sensory task, similar to the one used in our research. Altogether, such technical advances may allow the identification of key neuronal subpopulations which mediate sensation and information processing in the behaving animal.

7. Abbreviations

AP	action potential
CV	coefficient of variation
DC	direct current
Freq.	Frequency
FS	fast spiking
GABA	γ-aminobutyric acid
ION	infraorbital nerve
ISI	inter-spike interval
L	layer
l	lateral
max.	maximum
ms	milisecond
nA	nanoampere
Pom	posterior medial nucleus of the thalamus
Po	posterior group of the thalamus
Pr5	principal trigmental nucleus
P	p value
p	posterior
RS	regular spiking
s.d.	standard deviation
S1	primary somatosensory cortex
sp5c	caudal division of the spinal trigeminal complex
Sp5i	interpolar divison of the spinal trigeminal complex
Sp5o	oral divison of the spinal trigeminal complex
Sp5	spinal trigeminal complex
s	second
VPm	ventral posterior medial nucleus of the thalamus
μA	microampere

8. References

Abeles, M., Bergman, H., Margalit, E., and Vaadia, E. (1993). Spatiotemporal firing patterns in the frontal cortex of behaving monkeys. J. Neurophysiol. 70, 1629–1638.

Adrian, E.D. (1919). The response of human sensory nerves to currents of short duration. J. Physiol. (Lond.) 53, 70–85.

Afraz, S.R., Kiani, R., and Esteky, H. (2006). Microstimulation of inferotemporal cortex influences face categorization. Nature 442, 692–695.

Ahissar, E., Sosnik, R., and Haidarliu, S. (2000). Transformation from temporal to rate coding in a somatosensory thalamocortical pathway. Nature 406, 302–306.

Andrasfalvy, B.K., Zemelman, B.V., Tang, J., and Vaziri, A. (2010). Two-photon single-cell optogenetic control of neuronal activity by sculpted light. Proc Natl Acad Sci U S A 107, 11981–11986.

Armstrong-James, M., and Fox, K. (1987). Spatiotemporal convergence and divergence in the rat S1 "barrel" cortex. J. Comp. Neurol. 263, 265–281.

Asanuma, H. (1989). The Motor Cortex (Books on Demand).

Asanuma, H., and Sakata, H. (1967). Functional organization of a cortical efferent system examined with focal depth stimulation in cats. Journal of Neurophysiology 30, 35–54.

Bair, W., and Koch, C. (1996). Temporal precision of spike trains in extrastriate cortex of the behaving macaque monkey. Neural Comput 8, 1185–1202.

Bair, W., Koch, C., Newsome, W., and Britten, K. (1994). Power spectrum analysis of bursting cells in area MT in the behaving monkey. J. Neurosci. 14, 2870–2892.

Bartlett, J.R., and Doty, R.W. (1980). An exploration of the ability of macaques to detect microstimulation of striate cortex. Acta Neurobiol Exp (Wars) 40, 713–727.

Bonifazi, P., Goldin, M., Picardo, M.A., Jorquera, I., Cattani, A., Bianconi, G., Represa, A., Ben-Ari, Y., and Cossart, R. (2009). GABAergic hub neurons orchestrate synchrony in developing hippocampal networks. Science 326, 1419–1424.

Boyden, E.S., Zhang, F., Bamberg, E., Nagel, G., and Deisseroth, K. (2005). Millisecond-timescale, genetically targeted optical control of neural activity. Nat Neurosci 8, 1263–1268.

Brecht, M. (2007). Barrel cortex and whisker-mediated behaviors. Curr. Opin. Neurobiol. 17, 408–416.

Brecht, M., and Sakmann, B. (2002). Whisker maps of neuronal subclasses of the rat ventral posterior medial thalamus, identified by whole-cell voltage recording and morphological reconstruction. J. Physiol. (Lond.) 538, 495–515.

Brecht, M., Schneider, M., and Manns, I.D. (2005). Silent Neurons in Sensorimotor Cortices: Implications for Cortical Plasticity. In Neural Plasticity in Adult Somatic Sensory-motor Systems, (Philadelphia, PA, US: Taylor & Francis), pp. 1–19.

Brecht, M., Schneider, M., Sakmann, B., and Margrie, T.W. (2004). Whisker movements evoked by stimulation of single pyramidal cells in rat motor cortex. Nature 427, 704–710.

Britten, K.H., Newsome, W.T., Shadlen, M.N., Celebrini, S., and Movshon, J.A. (1996). A relationship between behavioral choice and the visual responses of neurons in macaque MT. Vis. Neurosci. 13, 87–100.

Brunel, N., and Hakim, V. (1999). Fast global oscillations in networks of integrate-and-fire neurons with low firing rates. Neural Comput 11, 1621–1671.

Butovas, S., and Schwarz, C. (2007). Detection psychophysics of intracortical microstimulation in rat primary somatosensory cortex. The European Journal of Neuroscience 25, 2161–2169.

Cardin, J.A., Carlen, M., Meletis, K., Knoblich, U., Zhang, F., Deisseroth, K., Tsai, L.H., and Moore, C.I. (2009). Driving fast-spiking cells induces gamma rhythm and controls sensory responses. Nature 459, 663–667.

Cattaneo, A., Maffei, L., and Morrone, C. (1981). Two firing patterns in the discharge of complex cells encoding different attributes of the visual stimulus. Exp Brain Res 43, 115–118.

Cohen, M.R., and Newsome, W.T. (2004). What electrical microstimulation has revealed about the neural basis of cognition. Curr. Opin. Neurobiol. 14, 169–177.

Connors, B.W., and Gutnick, M.J. (1990). Intrinsic firing patterns of diverse neocortical neurons. Trends in Neurosciences 13, 99–104.

Creutzfeldt, O.D. (1995). Cortex Cerebri: Performance, Structural and Functional Organisation of the Cortex (Oxford University Press).

Crick, F. (1984). Function of the thalamic reticular complex: the searchlight hypothesis. Proc. Natl. Acad. Sci. U.S.A. 81, 4586–4590.

Crochet, S., and Petersen, C.C. (2006). Correlating whisker behavior with membrane potential in barrel cortex of awake mice. Nat Neurosci 9, 608–610.

Van Der Loos, H. (1976). Barreloids in mouse somatosensory thalamus. Neurosci. Lett. 2, 1–6.

Diamond, M.E., Armstrong-James, M., and Ebner, F.F. (1993). Experience-dependent plasticity in adult rat barrel cortex. Proc. Natl. Acad. Sci. U.S.A. 90, 2082–2086.

Erzurumlu, R.S., Bates, C.A., and Killackey, H.P. (1980). Differential organization of thalamic projection cells in the brain stem trigeminal complex of the rat. Brain Res. 198, 427–433.

Fritsch, G., and Hitzig, E. (1870). Ueber die elektrische Erregbarkeit des Grosshirns. Arch. Anat. Physiol. Wiss. Med. 37, 300–332.

Gabbiani, F., Metzner, W., Wessel, R., and Koch, C. (1996). From stimulus encoding to feature extraction in weakly electric fish. Nature 384, 564–567.

Galarreta, M., and Hestrin, S. (1999). A network of fast-spiking cells in the neocortex connected by electrical synapses. Nature 402, 72–75.

Galarreta, M., and Hestrin, S. (2002). Electrical and chemical synapses among parvalbumin fast-spiking GABAergic interneurons in adult mouse neocortex. Proceedings of the National Academy of Sciences of the United States of America 99, 12438–12443.

Gibson, J.R., Beierlein, M., and Connors, B.W. (1999). Two networks of electrically coupled inhibitory neurons in neocortex. Nature 402, 75–79.

Goense, J., Ratnam, R., and Nelson, M. (2003). Burst firing improves the detection of weak signals in spike trains. Neurocomputing 52-54, 103–108.

Gray, C.M., and McCormick, D.A. (1996). Chattering cells: superficial pyramidal neurons contributing to the generation of synchronous oscillations in the visual cortex. Science 274, 109–113.

Greenberg, D.S., Houweling, A.R., and Kerr, J.N. (2008). Population imaging of ongoing neuronal activity in the visual cortex of awake rats. Nature Neuroscience 11, 749–751.

Gunaydin, L.A., Yizhar, O., Berndt, A., Sohal, V.S., Deisseroth, K., and Hegemann, P. (2010). Ultrafast optogenetic control. Nat. Neurosci. 13, 387–392.

Hahnloser, R.H., Kozhevnikov, A.A., and Fee, M.S. (2002). An ultra-sparse code underlies the generation of neural sequences in a songbird. Nature 419, 65–70.

Herfst, L.J., and Brecht, M. (2008). Whisker movements evoked by stimulation of single motor neurons in the facial nucleus of the rat. Journal of Neurophysiology 99, 2821–2832.

Houweling, A.R., and Brecht, M. (2008). Behavioural report of single neuron stimulation in somatosensory cortex. Nature 451, 65–68.

Houweling, A.R., Doron, G., Voigt, B.C., Herfst, L.J., and Brecht, M. (2010). Nanostimulation: manipulation of single neuron activity by juxtacellular current injection. J. Neurophysiol. 103, 1696–1704.

Hubel, D.H., and Wiesel, T.N. (1977). Ferrier lecture. Functional architecture of macaque monkey visual cortex. Proc. R. Soc. Lond., B, Biol. Sci. 198, 1–59.

Huber, D., Petreanu, L., Ghitani, N., Ranade, S., Hromadka, T., Mainen, Z., and Svoboda, K. (2008). Sparse optical microstimulation in barrel cortex drives learned behaviour in freely moving mice. Nature 451, 61–64.

Jacobs, A.L., Fridman, G., Douglas, R.M., Alam, N.M., Latham, P.E., Prusky, G.T., and Nirenberg, S. (2009). Ruling out and ruling in neural codes. Proceedings of the National Academy of Sciences of the United States of America 106, 5936–5941.

Jones, S.R., Pritchett, D.L., Stufflebeam, S.M., Hämäläinen, M., and Moore, C.I. (2007). Neural correlates of tactile detection: a combined magnetoencephalography and biophysically based computational modeling study. J. Neurosci. 27, 10751–10764.

Kapfer, C., Glickfeld, L.L., Atallah, B.V., and Scanziani, M. (2007). Supralinear increase of recurrent inhibition during sparse activity in the somatosensory cortex. Nature Neuroscience 10, 743–753.

Katona, G., Szalay, G., Maák, P., Kaszás, A., Veress, M., Hillier, D., Chiovini, B., Vizi, E.S., Roska, B., and Rózsa, B. (2012). Fast two-photon in vivo imaging with three-dimensional random-access scanning in large tissue volumes. Nature Methods 9, 201–208.

Kistler, W.M., and De Zeeuw, C.I. (2002). Dynamical working memory and timed responses: the role of reverberating loops in the olivo-cerebellar system. Neural Comput 14, 2597–2626.

Kwan, A.C., and Dan, Y. (2012). Dissection of Cortical Microcircuits by Single-Neuron Stimulation In Vivo. Current Biology: CB.

de Lafuente, V., and Romo, R. (2005). Neuronal correlates of subjective sensory experience. Nat. Neurosci. 8, 1698–1703.

Lak, A., Arabzadeh, E., and Diamond, M.E. (2008). Enhanced response of neurons in rat somatosensory cortex to stimuli containing temporal noise. Cereb Cortex 18, 1085–1093.

Larkum, M.E., Zhu, J.J., and Sakmann, B. (1999). A new cellular mechanism for coupling inputs arriving at different cortical layers. Nature 398, 338–341.

LeChasseur, Y., Dufour, S., Lavertu, G., Bories, C., Deschênes, M., Vallée, R., and Koninck, Y.D. (2011). A microprobe for parallel optical and electrical recordings from single neurons in vivo. Nature Methods 8, 319–325.

Lee, A.K., Manns, I.D., Sakmann, B., and Brecht, M. (2006). Whole-cell recordings in freely moving rats. Neuron 51, 399–407.

Lesica, N.A., and Stanley, G.B. (2004). Encoding of natural scene movies by tonic and burst spikes in the lateral geniculate nucleus. J. Neurosci. 24, 10731–10740.

Lewicki, M.S., and Konishi, M. (1995). Mechanisms underlying the sensitivity of songbird forebrain neurons to temporal order. Proc. Natl. Acad. Sci. U.S.A. 92, 5582–5586.

Li, C.Y., Poo, M.M., and Dan, Y. (2009). Burst spiking of a single cortical neuron modifies global brain state. Science 324, 643–646.

Lichtenstein, S.H., Carvell, G.E., and Simons, D.J. (1990). Responses of rat trigeminal ganglion neurons to movements of vibrissae in different directions. Somatosens Mot Res 7, 47–65.

Linkenkaer-Hansen, K., Nikulin, V.V., Palva, S., Ilmoniemi, R.J., and Palva, J.M. (2004). Prestimulus oscillations enhance psychophysical performance in humans. J. Neurosci. 24, 10186–10190.

Lisman, J.E. (1997). Bursts as a unit of neural information: making unreliable synapses reliable. Trends in Neurosciences 20, 38–43.

Livingstone, M.S., Freeman, D.C., and Hubel, D.H. (1996). Visual responses in V1 of freely viewing monkeys. Cold Spring Harb. Symp. Quant. Biol. 61, 27–37.

Luna, R., Hernandez, A., Brody, C.D., and Romo, R. (2005). Neural codes for perceptual discrimination in primary somatosensory cortex. Nature Neuroscience 8, 1210–1219.

Ma, P.M. (1991). The barrelettes--architectonic vibrissal representations in the brainstem trigeminal complex of the mouse. I. Normal structural organization. J. Comp. Neurol. 309, 161–199.

Mainen, Z.F., and Sejnowski, T.J. (1995). Reliability of spike timing in neocortical neurons. Science 268, 1503–1506.

Margrie, T.W., Brecht, M., and Sakmann, B. (2002). In vivo, low-resistance, whole-cell recordings from neurons in the anaesthetized and awake mammalian brain. Pflugers Arch 444, 491–498.

Marsat, G., and Pollack, G.S. (2006). A behavioral role for feature detection by sensory bursts. J. Neurosci. 26, 10542–10547.

Mateo, C., Avermann, M., Gentet, L.J., Zhang, F., Deisseroth, K., and Petersen, C.C. (2011). In Vivo optogenetic stimulation of neocortical excitatory neurons drives brain-state-dependent inhibition. Curr Biol 21, 1593–1602.

Metzner, W., Koch, C., Wessel, R., and Gabbiani, F. (1998). Feature extraction by burst-like spike patterns in multiple sensory maps. J. Neurosci. 18, 2283–2300.

Murphey, D.K., and Maunsell, J.H. (2007). Behavioral detection of electrical microstimulation in different cortical visual areas. Curr Biol 17, 862–867.

Nowak, L.G., Azouz, R., Sanchez-Vives, M.V., Gray, C.M., and McCormick, D.A. (2003). Electrophysiological classes of cat primary visual cortical neurons in vivo as revealed by quantitative analyses. J. Neurophysiol. 89, 1541–1566.

Olshausen, B.A., and Field, D.J. (2004). Sparse coding of sensory inputs. Curr. Opin. Neurobiol. 14, 481–487.

Oswald, A.-M.M., Chacron, M.J., Doiron, B., Bastian, J., and Maler, L. (2004). Parallel processing of sensory input by bursts and isolated spikes. J. Neurosci. 24, 4351–4362.

Otto, T., Eichenbaum, H., Wiener, S.I., and Wible, C.G. (1991). Learning-related patterns of CA1 spike trains parallel stimulation parameters optimal for inducing hippocampal long-term potentiation. Hippocampus 1, 181–192.

Papadopoulou, M., Cassenaer, S., Nowotny, T., and Laurent, G. (2011). Normalization for sparse encoding of odors by a wide-field interneuron. Science 332, 721–725.

Penfield, W., and Boldery, P. (1937). Somatic motor and sensory representation in the cerebral cortex of man as studied by electrical stimulation. Brain 60, 389–443.

Perkins, K.L. (2006). Cell-attached voltage-clamp and current-clamp recording and stimulation techniques in brain slices. J. Neurosci. Methods 154, 1–18.

Petersen, C.C.H. (2007). The functional organization of the barrel cortex. Neuron 56, 339–355.

Pierret, T., Lavallée, P., and Deschênes, M. (2000). Parallel streams for the relay of vibrissal information through thalamic barreloids. J. Neurosci. 20, 7455–7462.

Pinault, D. (1994). Golgi-like labeling of a single neuron recorded extracellularly. Neurosci Lett 170, 255–260.

Pinault, D. (1996). A novel single-cell staining procedure performed in vivo under electrophysiological control: morpho-functional features of juxtacellularly labeled thalamic cells and other central neurons with biocytin or Neurobiotin. J Neurosci Methods 65, 113–136.

Ragan, T., Kadiri, L.R., Venkataraju, K.U., Bahlmann, K., Sutin, J., Taranda, J., Arganda-Carreras, I., Kim, Y., Seung, H.S., and Osten, P. (2012). Serial two-photon tomography for automated ex vivo mouse brain imaging. Nat. Methods 9, 255–258.

Rancz, E.A., Franks, K.M., Schwarz, M.K., Pichler, B., Schaefer, A.T., and Margrie, T.W. (2011). Transfection via whole-cell recording in vivo: bridging single-cell physiology, genetics and connectomics. Nat. Neurosci. 14, 527–532.

Rickgauer, J.P., and Tank, D.W. (2009). Two-photon excitation of channelrhodopsin-2 at saturation. Proc. Natl. Acad. Sci. U.S.A. 106, 15025–15030.

Romo, R., Hernandez, A., Zainos, A., and Salinas, E. (1998). Somatosensory discrimination based on cortical microstimulation. Nature 392, 387–390.

Salzman, C.D., Britten, K.H., and Newsome, W.T. (1990). Cortical microstimulation influences perceptual judgements of motion direction. Nature 346, 174–177.

Schmidt, E.M., Bak, M.J., Hambrecht, F.T., Kufta, C.V., O'Rourke, D.K., and Vallabhanath, P. (1996). Feasibility of a visual prosthesis for the blind based on intracortical microstimulation of the visual cortex. Brain 119, 507–522.

Schoenenberger, P., Grunditz, A., Rose, T., and Oertner, T.G. (2008). Optimizing the spatial resolution of Channelrhodopsin-2 activation. Brain Cell Biol 36, 119–127.

Schubert, R., Haufe, S., Blankenburg, F., Villringer, A., and Curio, G. (2009). Now you'll feel it, now you won't: EEG rhythms predict the effectiveness of perceptual masking. J Cogn Neurosci 21, 2407–2419.

Shadlen, M.N., and Newsome, W.T. (1994). Noise, neural codes and cortical organization. Current Opinion in Neurobiology 4, 569–579.

Shadlen, M.N., and Newsome, W.T. (1998). The variable discharge of cortical neurons: implications for connectivity, computation, and information coding. J. Neurosci. 18, 3870–3896.

Silberberg, G., and Markram, H. (2007). Disynaptic inhibition between neocortical pyramidal cells mediated by Martinotti cells. Neuron 53, 735–746.

Simons, D.J. (1978). Response properties of vibrissa units in rat SI somatosensory neocortex. J. Neurophysiol. 41, 798–820.

Softky, W.R., and Koch, C. (1993). The highly irregular firing of cortical cells is inconsistent with temporal integration of random EPSPs. J. Neurosci. 13, 334–350.

Steriade, M., Timofeev, I., and Grenier, F. (2001). Natural waking and sleep states: a view from inside neocortical neurons. J Neurophysiol 85, 1969–1985.

Stoney, S.D., Thompson, W.D., and Asanuma, H. (1968). Excitation of pyramidal tract cells by intracortical microstimulation: effective extent of stimulating current. J Neurophysiol 31, 659–669.

Swadlow, H.A. (2003). Fast-spike interneurons and feedforward inhibition in awake sensory neocortex. Cereb Cortex 13, 25–32.

Tehovnik, E.J., Slocum, W.M., and Schiller, P.H. (2003). Saccadic eye movements evoked by microstimulation of striate cortex. Eur J Neurosci 17, 870–878.

Vallbo, A.B., Olsson, K.A., Westberg, K.G., and Clark, F.J. (1984). Microstimulation of single tactile afferents from the human hand. Sensory attributes related to unit type and properties of receptive fields. Brain 107, 727–749.

Veinante, P., and Deschênes, M. (1999). Single- and multi-whisker channels in the ascending projections from the principal trigeminal nucleus in the rat. J. Neurosci. 19, 5085–5095.

Voigt, B.C., Brecht, M., and Houweling, A.R. (2008). Behavioral detectability of single-cell stimulation in the ventral posterior medial nucleus of the thalamus. J Neurosci 28, 12362–12367.

van Vreeswijk, C., and Sompolinsky, H. (1996). Chaos in neuronal networks with balanced excitatory and inhibitory activity. Science 274, 1724–1726.

Welker, C. (1971). Microelectrode delineation of fine grain somatotopic organization of (SmI) cerebral neocortex in albino rat. Brain Res. 26, 259–275.

Wolfe, J., Houweling, A.R., and Brecht, M. (2010). Sparse and powerful cortical spikes. Current Opinion in Neurobiology 20, 306–312.

Woolsey, T.A., and Van der Loos, H. (1970). The structural organization of layer IV in the somatosensory region (SI) of mouse cerebral cortex. The description of a cortical field composed of discrete cytoarchitectonic units. Brain Res. 17, 205–242.

Yu, C., Derdikman, D., Haidarliu, S., and Ahissar, E. (2006). Parallel thalamic pathways for whisking and touch signals in the rat. PLoS Biol. 4, e124.

Zhang, F., Wang, L.P., Brauner, M., Liewald, J.F., Kay, K., Watzke, N., Wood, P.G., Bamberg, E., Nagel, G., Gottschalk, A., et al. (2007). Multimodal fast optical interrogation of neural circuitry. Nature 446, 633–639.

9. Acknowledgements

I would never have been able to finish my dissertation without the guidance of my supervisor, help from colleagues and friends, and support from my family. I would like to express my deepest gratitude to my supervisor, Prof. Michael Brecht, for his excellent guidance and for providing me with an excellent atmosphere for doing research. His wisdom, knowledge and commitment to the highest standards inspired and motivated me. I would like to thank my colleagues and friends in the Brecht lab:

- Dr. Arthur Houweling, who let me experience the research of single-neuron detection in the awake rat and helped me with practical issues beyond the textbooks and patiently corrected my writing and analysis.
- Dr. Birgit Voigt, who handed me over her experimental setup in a perfect condition as well as guided me throughout countless technical and methodological issues. Her kind assistance saved me precious hours and days of troubleshooting and maintenance.
- Dr. Moritz von Heimendahl, who as a good friend and an excellent mentor, was always willing to help and give me his best suggestions. His guidance and ideas regarding data organization and analysis yielded key findings and insights in my research, and for that I am forever grateful to him.
- Dr. Edith Chorev, who is one of the most talented electrophysiologists I ever met. Her professional tips and technical expertise helped me to solve many seemingly insurmountable problems and her endless knowledge deepened my understanding in neurophysiology and neuroscience.
- Dr. Andrea Burgalossi and Dr. Rajnish Rao who carefully went over my manuscript and provided many useful comments and advices which greatly improved it.
- Brigitte Geue and Undine Schneeweiss, our extraordinary lab technicians who were like two mothers to me and provided beside of excellent technical services a lot of caring and support. Their wisdom and practical solutions to countless problems were invaluable to me.
- The rest of the Brecht lab team which were always so friendly and willing to help with any possible issue, making this period of my life unforgettable.

I would also like to thank my parents and sisters. They were always supporting me and encouraging me with their best wishes.

Finally, I would like to thank my wife, Ilana Altman-Doron and my daughter Eliya. They were always there cheering me up and stood by me through the countless lost weekends. Ilana, your love, support and constant patience taught me a lot about sacrifice and compromise. Eliya, your everlasting optimism and cheerfulness inspires me and teaches me daily important lessons about life.

This dissertation is dedicated to Ilana and Eliya, the two most wonderful people in my life.

10. Selbständigkeitserklärung

Ich erkläre hiermit, dass ich die vorliegende Arbeit ohne fremde Hilfe selbständig verfasst und keine anderen als die im Quellenverzeichnis angegebenen Hilfsmittel verwendet habe.

Ich erkläre weiterhin, dass ich alles gedanklich, inhaltlich oder wörtlich von anderen (z.B. aus Büchern, Zeitschriften, Zeitungen, Lexika, Internet usw.) Übernommene als solches kenntlich gemacht und gemäß den mir bekannten gängigen wissenschaftlichen Regeln korrekt zitiert, d.h. die jeweilige Herkunft im Text oder in den Anmerkungen belegt habe. Dies gilt gegebenenfalls auch für Tabellen, Skizzen, Zeichnungen, bildliche Darstellungen usw.

Ich nehme zur Kenntnis, dass die – auch zu einem späteren Zeitpunkt – nachgewiesene Unterlassung der Herkunftsangabe, das Fehlen von Zitationshinweisen, als versuchte Täuschung bzw. als Plagiat („geistiger Diebstahl“) gewertet werden wird.

Ich erkenne hiermit an, dass bei Vorliegen eines Plagiats die Arbeit nicht als selbstständige Leistung gewertet werden wird mit der Folge, dass mein Anspruch auf einen Leistungsnachweis entfällt.